Recent Progress of Bismuth Shielding Integral Experiments at China Institute of Atomic Energy

YangBo-Nie, ShiYu-Zhang, YanYan-Ding, Qi-Zhao, KuoZhi-Xu, XinYi-Pan

ShiYu-Zhang

Key Laboratory of Nuclear Data
China Nuclear Data Center(CNDC)
China Institute of Atomic Energy(CIAE)
Lanzhou Univeristy(LZU)
Beijing 102413, P.R.China
E-Mail: zsy20821@126.com

Contents

The Use of Nuclear Data

Data Measurement
Nuclear structure data,
Nuclear reaction data,
Benchmark experiment
……

Model theory
Nuclear reaction、
Nuclear structure……

Nuclear data libraries
-Experimental nuclear database
-Evaluated nuclear database
-Dedicated nuclear database

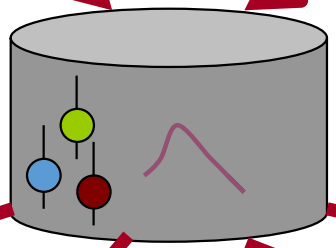

Scientific research:
Nuclear physics,
Nuclear reactor physics ……

Nuclear technology application:
Nuclear medicine,
Nuclear detection technology……

Nuclear energy development:
Nuclear power,
Nuclear fuel cycle……

Public education:
Science education,
Professional Education……

➢**The precision and reliability of nuclear data are directly related to the quality of nuclear engineering products and the application of nuclear technology**

Nuclear Data Production

Reaction and Structure theory

Fundamental experimental data

Basic study of nuclear physics

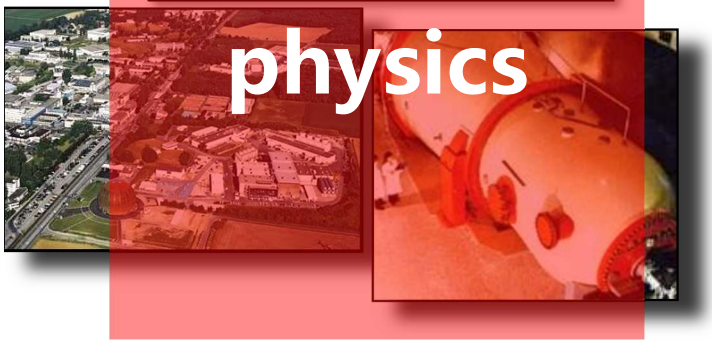

Modeling codes predictions

Evaluations

Data Processing

Application libraries

Transport simulation of integral experiments

Feedback

Integral experimental data

Check the quality of nuclear data

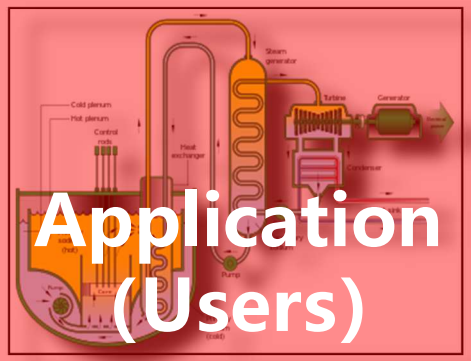

Application (Users)

Engineering design

Integral experiment is an essential part of evaluating nuclear data before it is provided to users.

CIAE Integral Experiment Arrangement

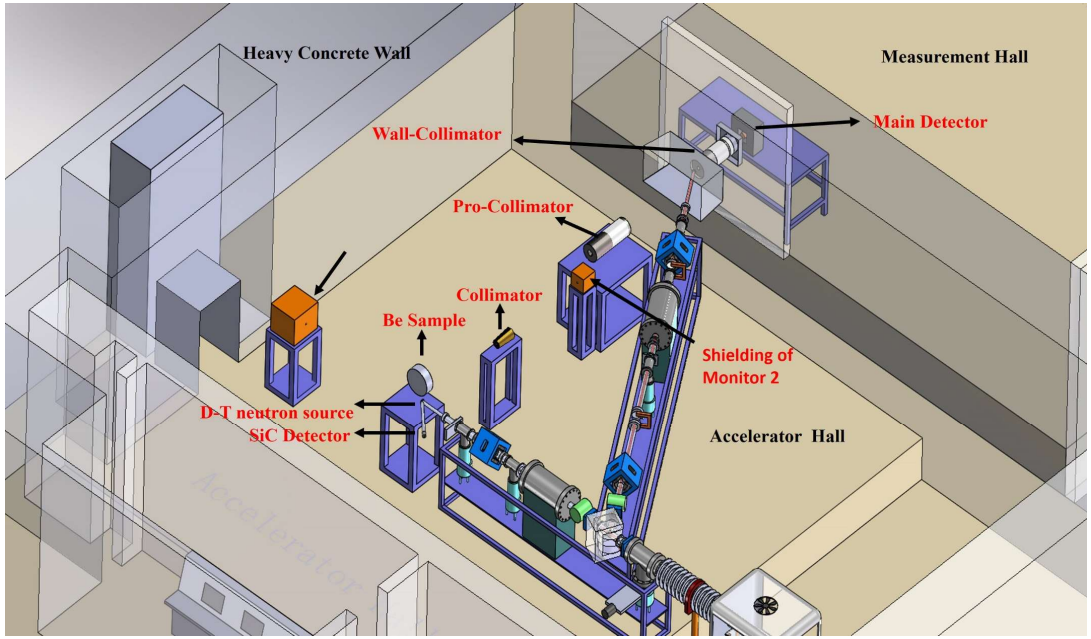

Measure TOF spectra of leakage neutrons at >90°.
Effect/background ratio reaches top international level.

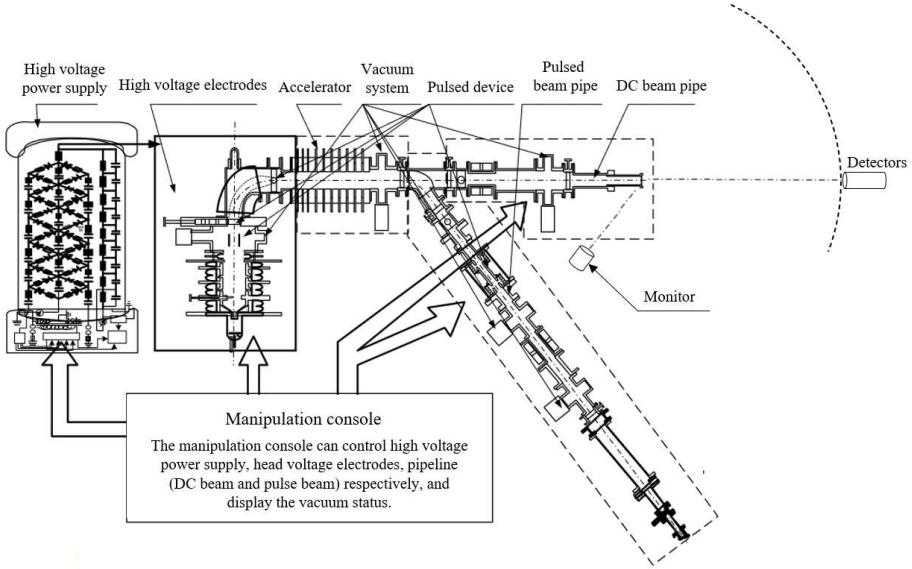

Table1. The integral experiments have been performed at CIAE

Sample	Size（cm）	Thickness（cm）	Degree（°）
^{238}U	10×10	5	45、135
	10×10	2，5，11	60、120
	30×30	3，6，9	60、120
Be	10×10	5，11	60、120
	ϕ30	4.4，8.8，13.2	47、58、72、108、122、133
Fe	ϕ13	5，10，15	60、120
	30×30		
^{nat}Ga	ϕ13	3.2，6.4	60、120
^{nat}W	10×10	3.5，7	60、120
C	ϕ13	20	60、120
SiC	ϕ13	20	60、120
Pb	ϕ13	5	60
	30×30	5，10，15	60、120
Pb-Bi	ϕ13	5	60
ThO_2	ϕ13	5.4，10.8	60、120
H_2O	ϕ13	5.2	60
Nb	ϕ13	5，10，15	60、120
Bi	30×30	5，10，15	60、120
	30×30	5，10，15	47、58、72、108、122、133
Zr	30×30	6，12，18	47、58、72、108、122、133

Current Focus of Shielding Integral Experiments

Current integral experiments focus on higher-precision measurements under diverse experimental conditions .

The platform upgrade to enable higher-precision TOF measurements.

Experiments were performed with both slab and spherical samples: the slab sample used three thicknesses at six detection angles, while the spherical sample used three thicknesses.

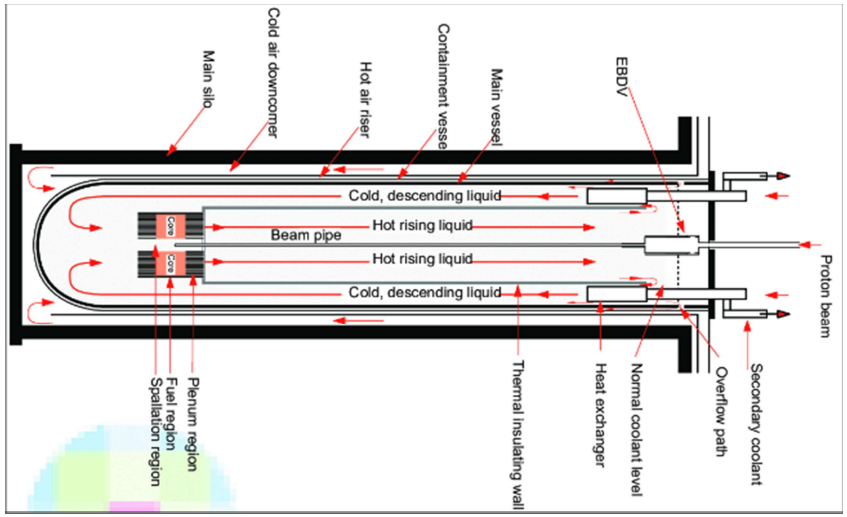

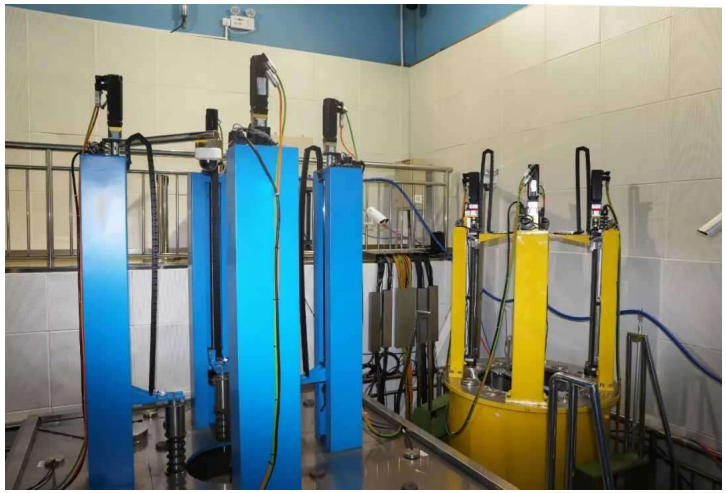

Bismuth

Component of **Pb-Bi eutectic coolant**
Applied in **lead-cooled fast reactors (LFRs)** and **ADS**

Experimental Platform– Bi Slab Sample

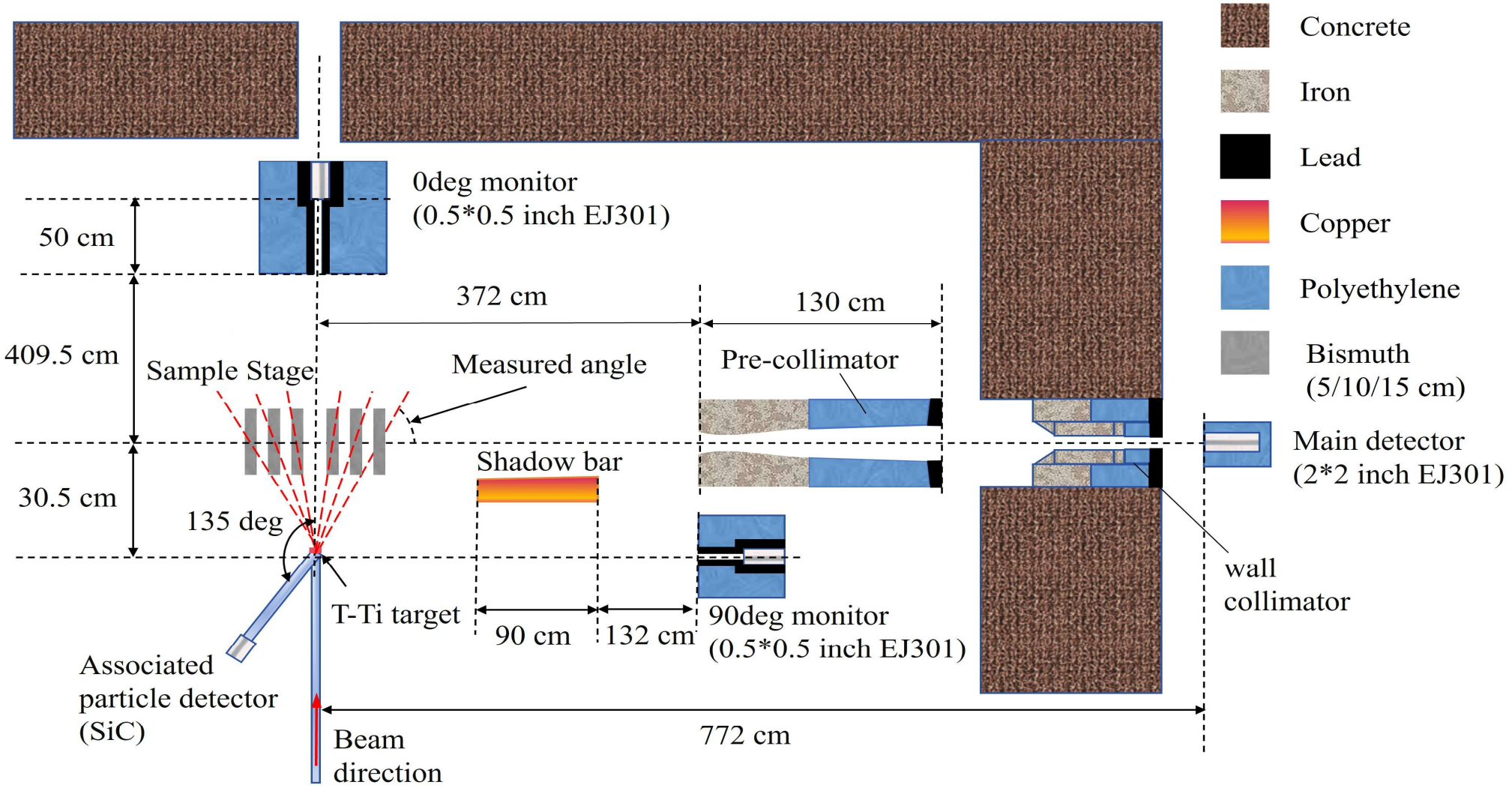

Neutron leakage spectra were measured for Bi samples of three thicknesses (5/10/15 × 30 × 30 cm) at six scattering angles (47° /58° /73° /107° /122° /133°).

Experimental Platform Upgrades for High-Precision TOF Measurements

① Digital Electronics & Full Waveform Recording

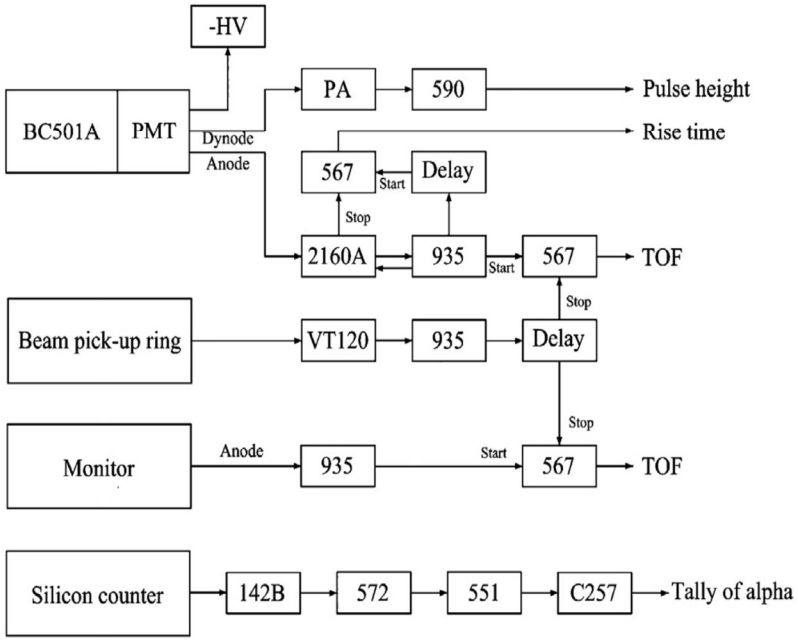

Parameter	Value
Number of Channels	16
Sampling Rate	500 MS/s
Resolution	12 bit
Max Acquisition Time per Waveform	20 μs
Data Transfer Rate	10^9 MS/s

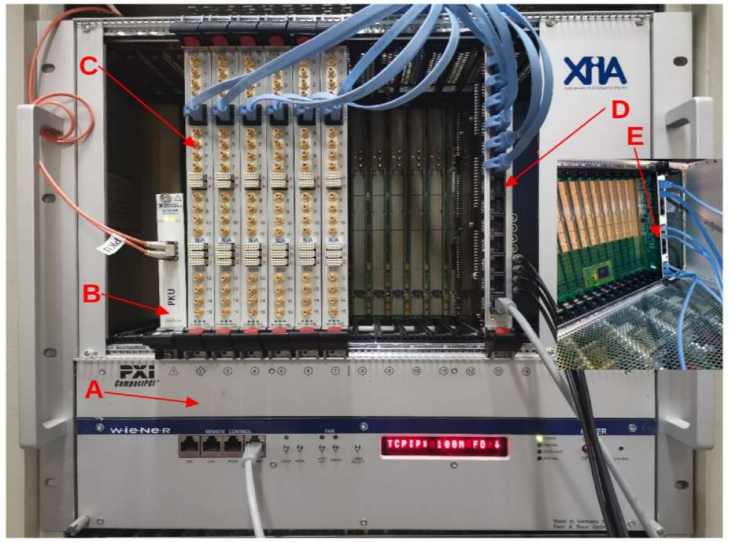

①Replaced traditional analog electronics with digitized acquisition system;

②Enables full waveform recording for advanced data processing and analysis.

② Accurate Pulse Time Distribution Shape Monitoring with Liquid Scintillator

① Liquid scintillator monitor + deconvolution algorithm;

② Neutron TOF spectra were preferred over gamma due to lower background and higher accuracy.

Response matrix

$$\begin{bmatrix} N_1 \\ N_2 \\ N_3 \\ \vdots \\ N_i \end{bmatrix} = \begin{bmatrix} R_{11} & R_{12} & R_{13} & \cdots & R_{1j} \\ R_{21} & R_{22} & R_{23} & \cdots & R_{2j} \\ R_{31} & R_{32} & R_{33} & \cdots & R_{3j} \\ \vdots & \vdots & \vdots & \ddots & \vdots \\ R_{i1} & R_{i2} & R_{i3} & \cdots & R_{ij} \end{bmatrix} \bullet \begin{bmatrix} \phi_1 \\ \phi_2 \\ \phi_3 \\ \vdots \\ \phi_j \end{bmatrix}$$

Neutron TOF Pulse time distribution

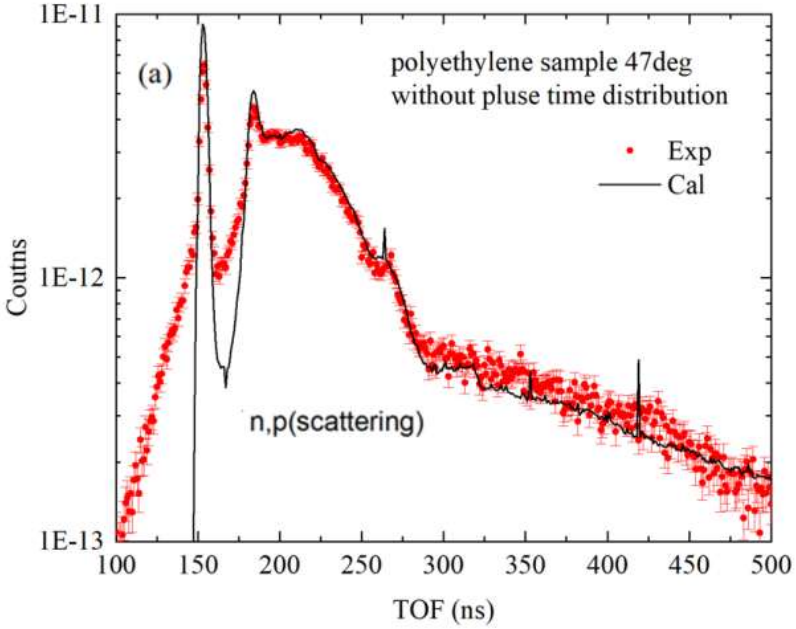

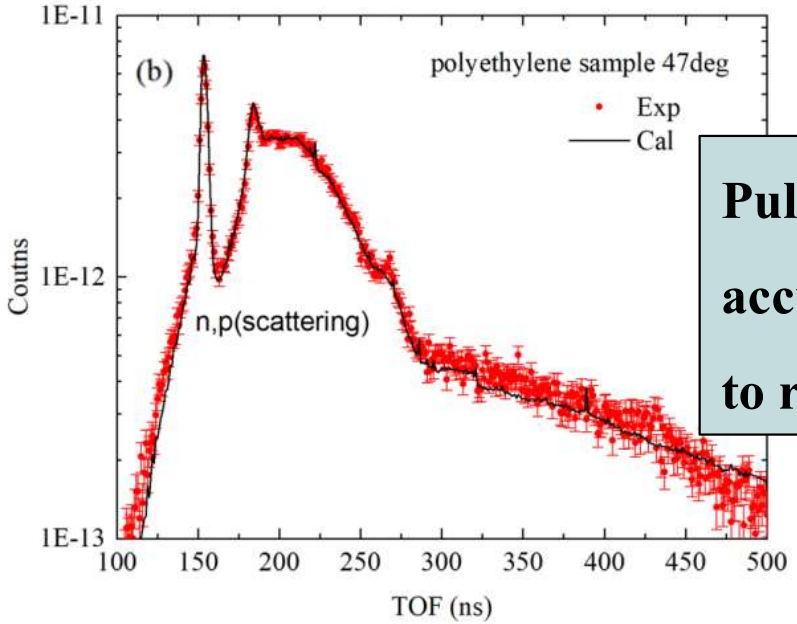

Pulse time profile accuracy is critical to result reliability.

③ Associated Particle Detection with SiC Detector

D-D neutrons inevitably accompany D-T sources due to deuteron beam deposition in the target.

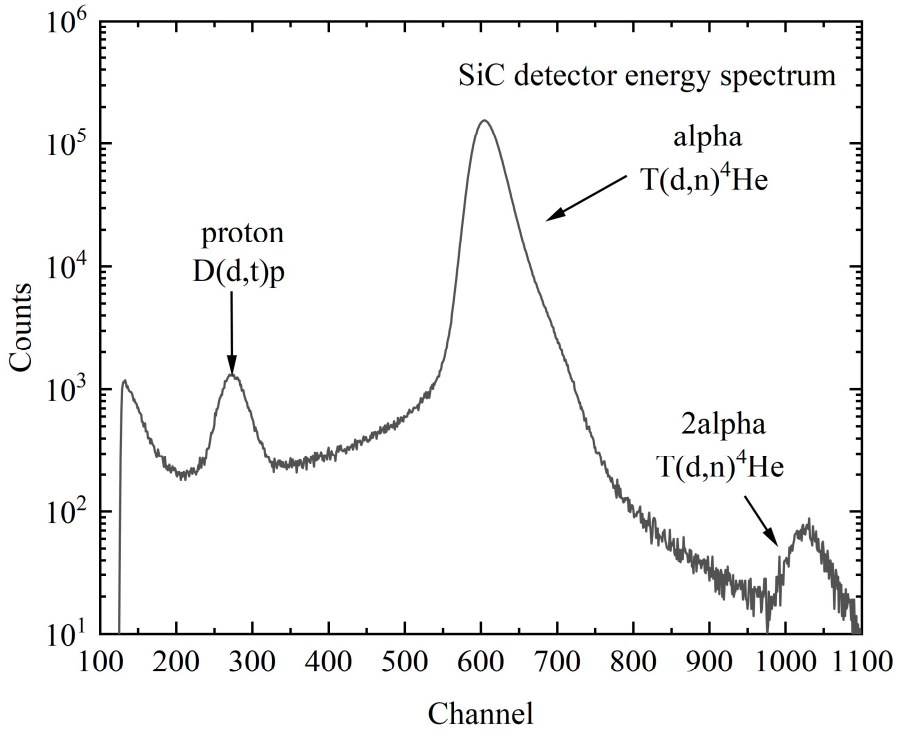

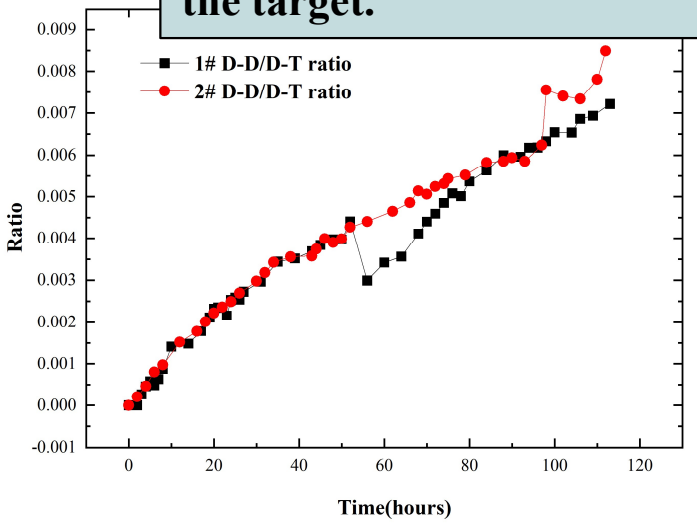

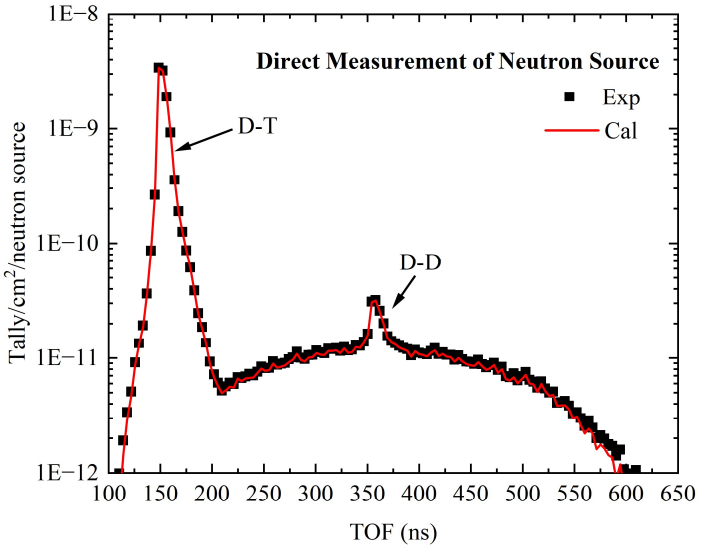

① SiC detector distinguishes DD-protons and DT-alphas;

② Enables accurate assessment of DD/DT neutron field composition.

Experimental Results – Standard Sample (CH_2)

2 Angles + 2 Conditions

① verify the accuracy and repeatability of the system.

② the n–p scattering cross section is internationally recognized.

③Systematic uncertainty < 3%.

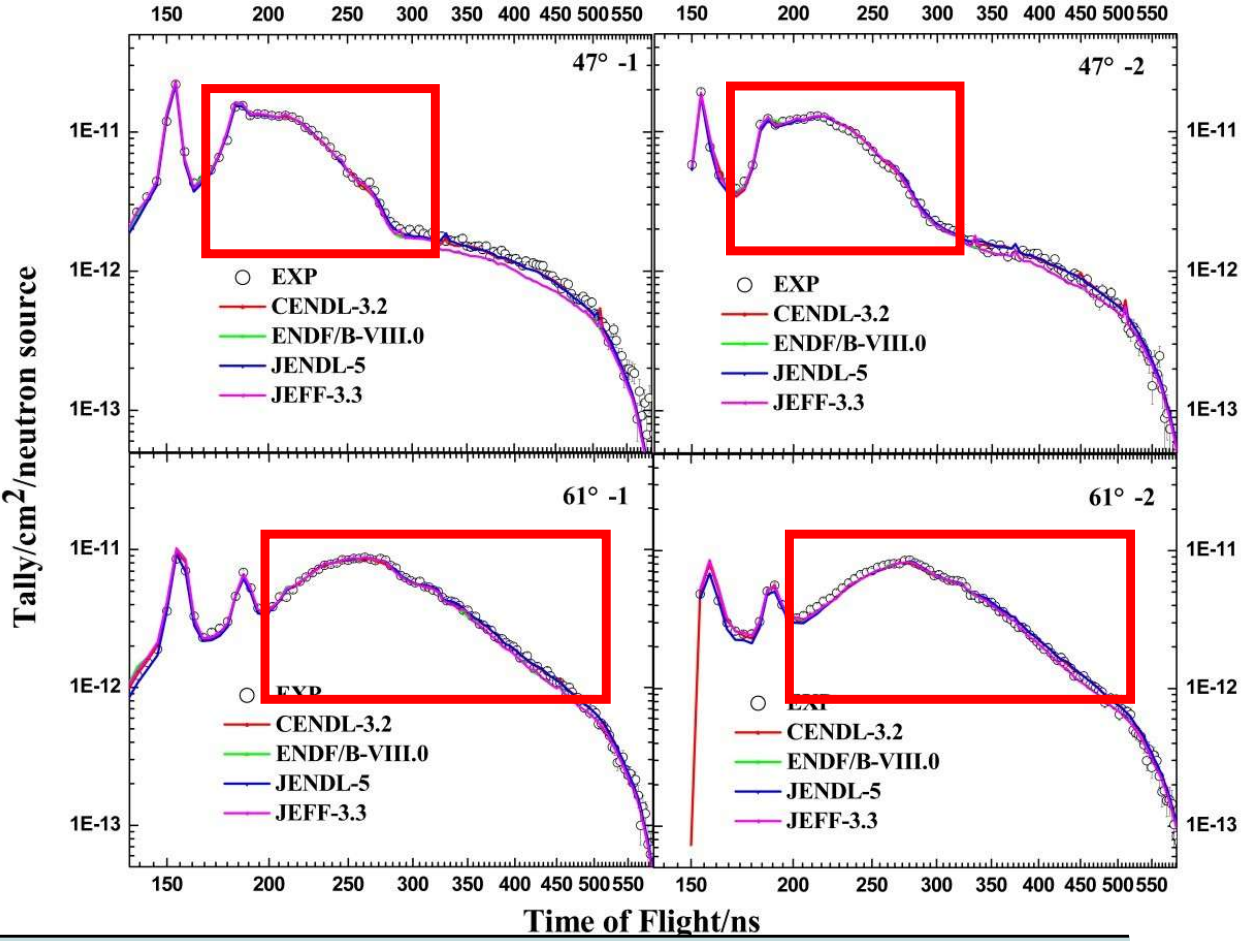

Angle	C/E value											
	CENDL-3.2			ENDF/B-VIII.0			JEDNL-5.0			JEFF-3.3		
47deg-1	0.9811	±	0.0298	0.9884	±	0.0300	0.9738	±	0.0296	0.9902	±	0.0301
47deg-2	1.0013	±	0.0304	1.0110	±	0.0307	1.0057	±	0.0306	1.0131	±	0.0308
61deg-1	0.9882	±	0.0299	0.9695	±	0.0293	0.9961	±	0.0301	0.9677	±	0.0292
61deg-2	0.9931	±	0.0301	0.9942	±	0.0301	1.0046	±	0.0304	0.9946	±	0.0301

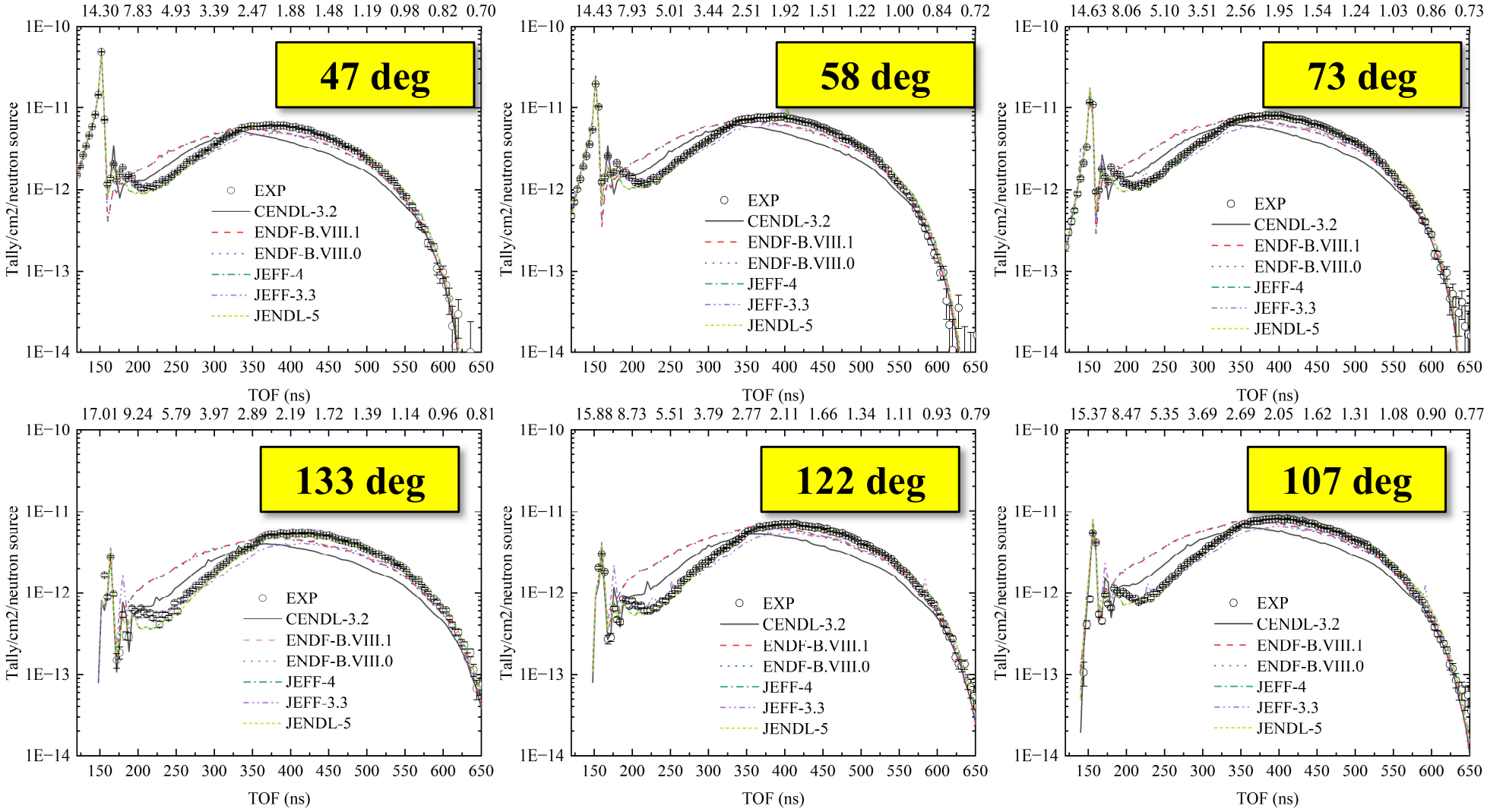

Experimental results for a 5cm thickness

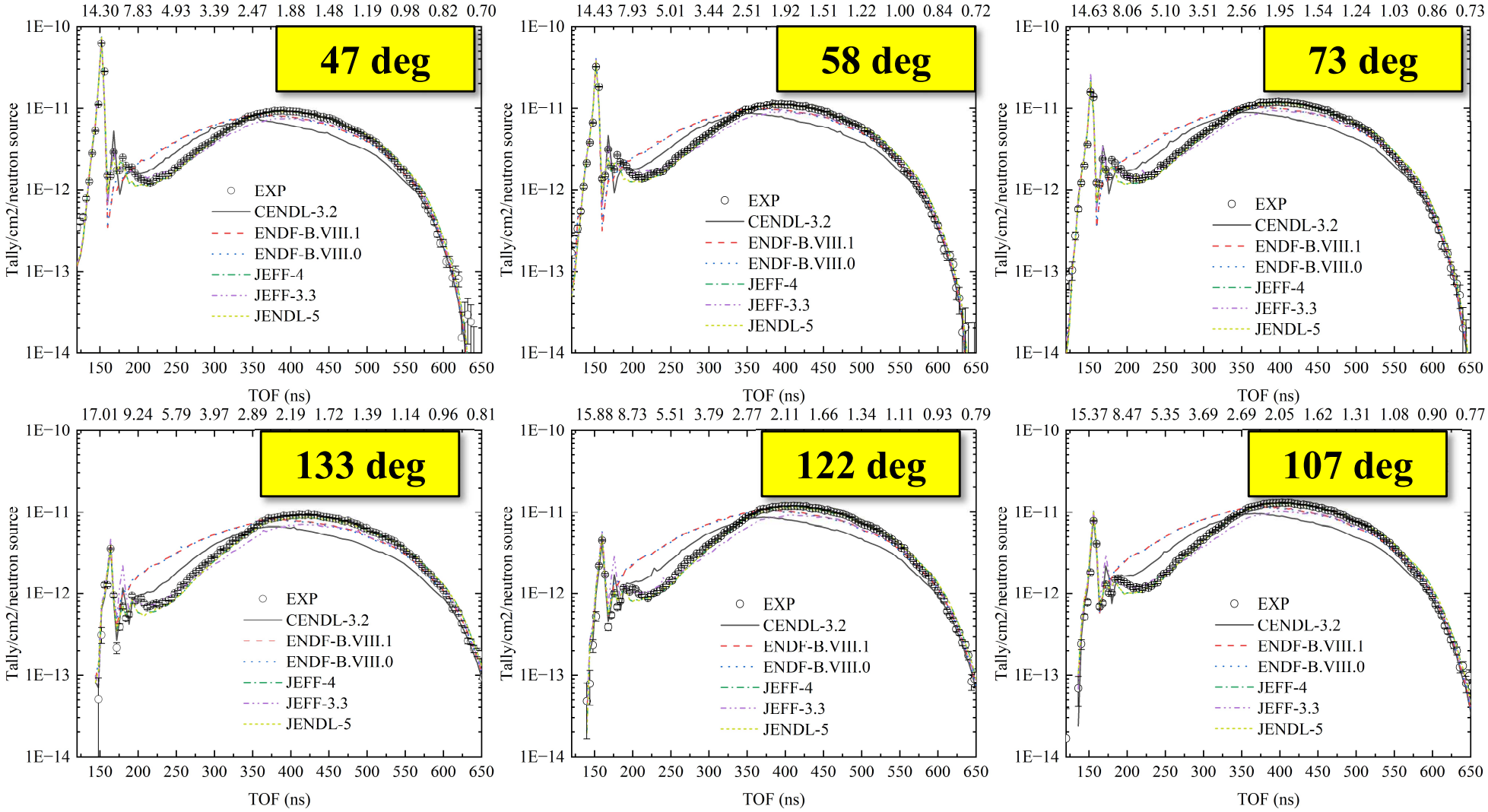

Experimental results for a 10cm thickness

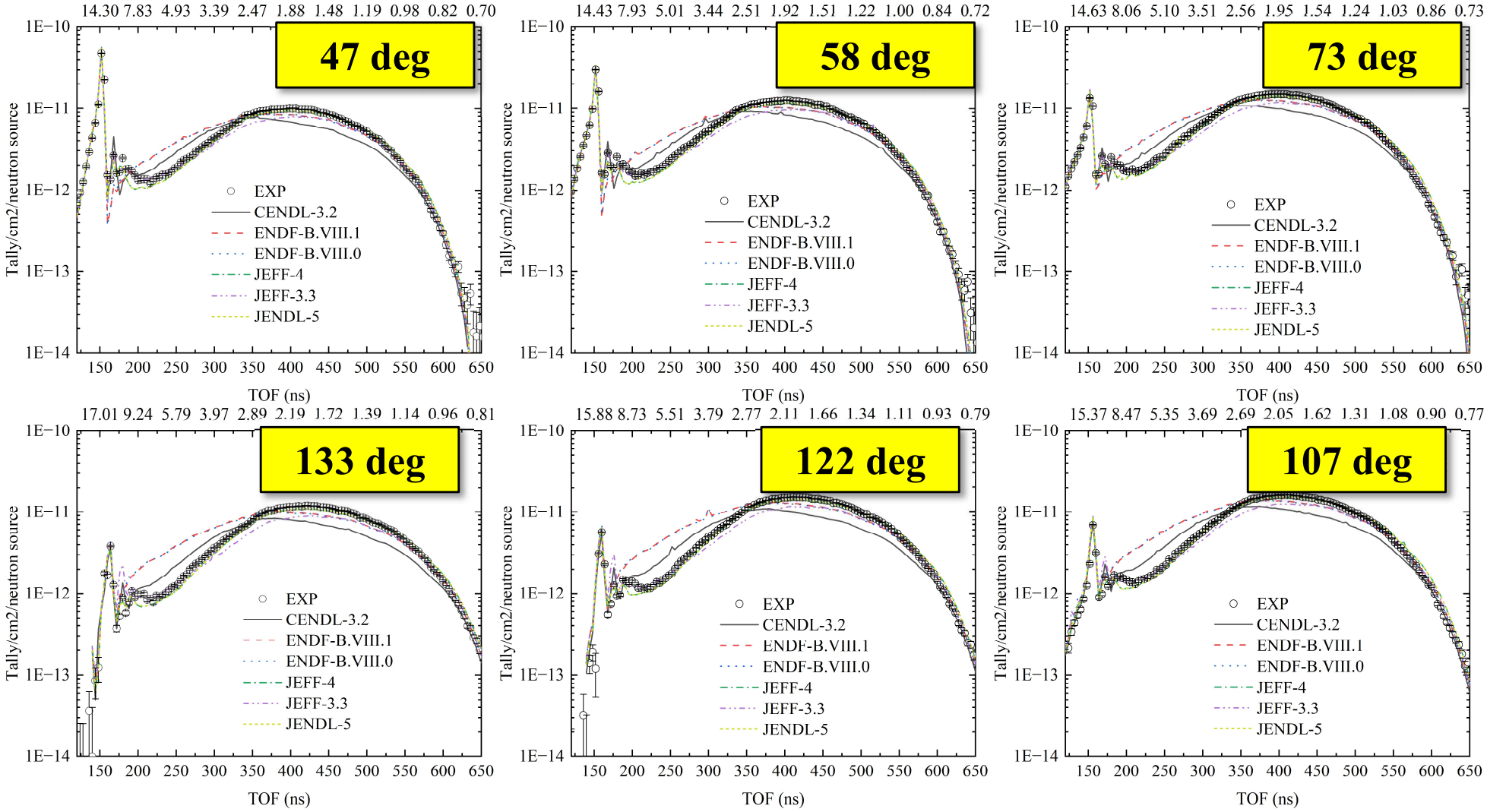

Experimental results for a 15cm thickness

Reaction Channel Separation in TOF Spectra

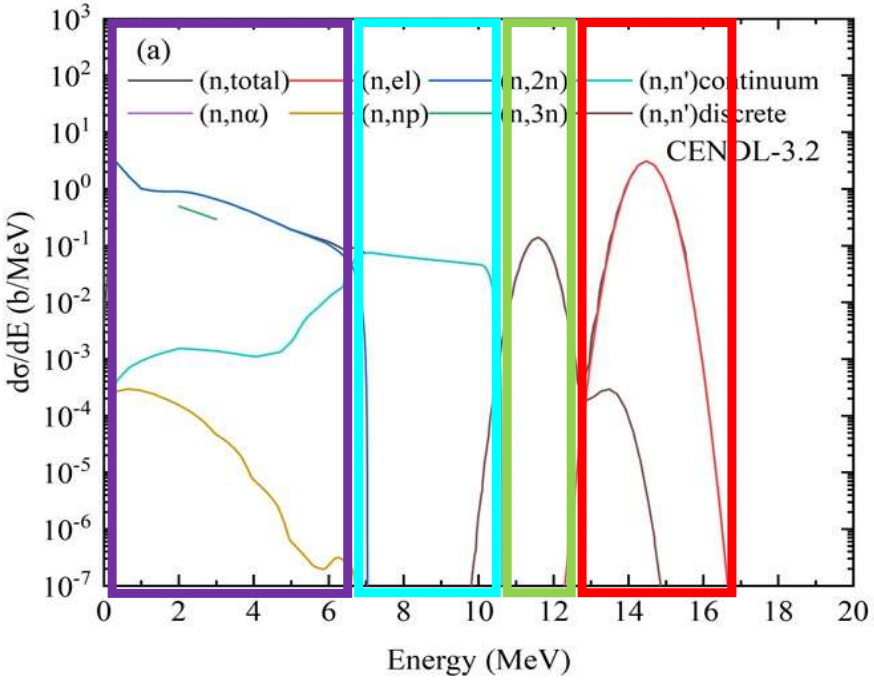

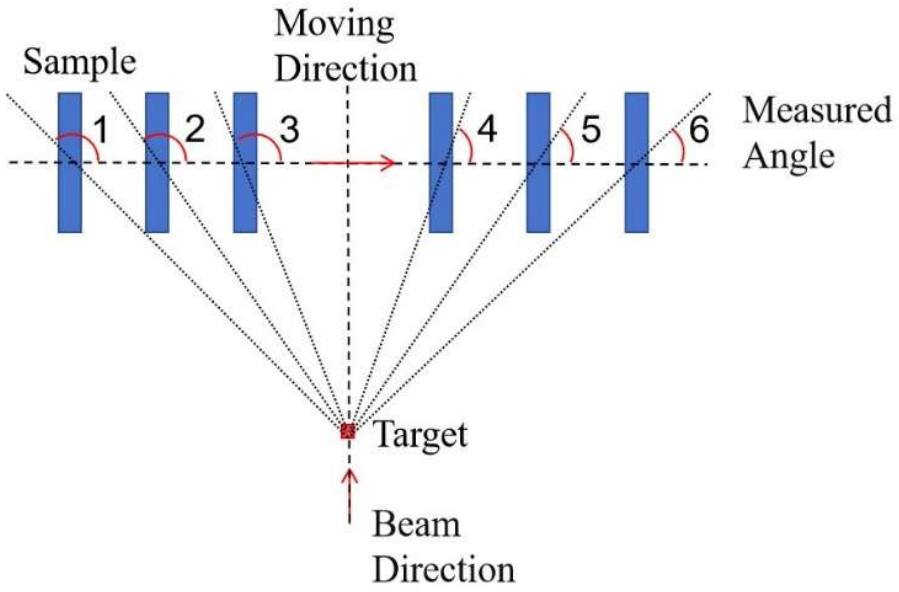

(n,2n) (n,inl)C

(n,inl)D (n,el)

①Energy regions are defined by the dominant contribution within that range.;

② TOF windows are determined by combining flight distance and energy intervals.

Bi Experimental Results Analysis (CENDL-3.2)

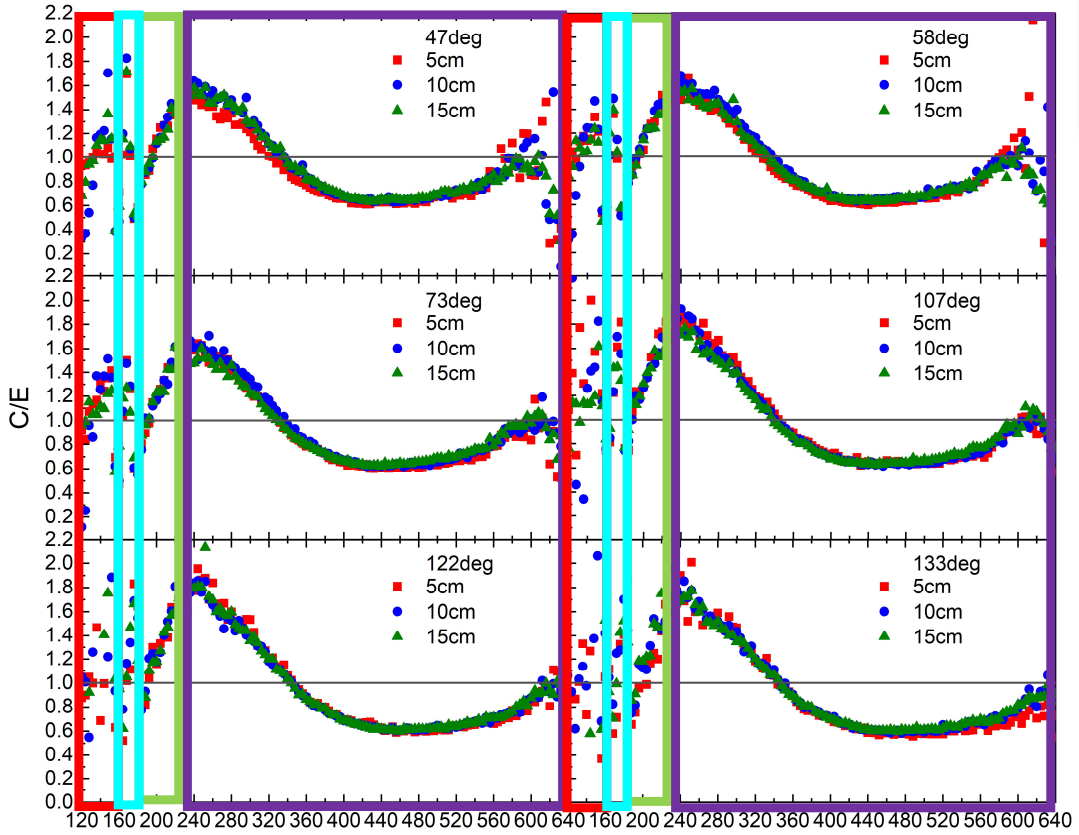

Angle (deg)	TOF (ns)			
	(n,el)	(n,n')discrete	(n,n')continuum	(n,2n)
47	132~156	160~172	176~216	220~608
58	132~160	160~172	176~216	220~616
73	132~160	164~176	180~220	224~624
107	140~160	164~176	180~224	228~636
122	144~164	168~180	184~228	232~644
133	148~168	172~184	188~232	236~652

C/E values across three different thicknesses show excellent consistency.

- **Elastic Region**

C/E values increase with angle; best performance at 133° , with minimal overlap from inelastic scattering.

- **Discrete-Level Inelastic Region**

Consistently overestimates across all angles but maintains a reasonable angular trend.

- **Continuous-Level Inelastic Region**

Accurate at small angles (47° , 58°), slightly overestimates at 73° , and more significantly at large angles.

- **(n,2n) Region:**

Systematically underestimates across the entire energy range.

C/E values by energy region for different nuclear data libraries at 5 cm thickness.

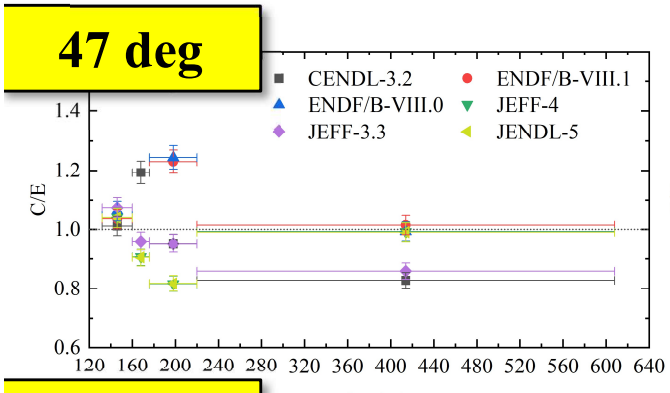

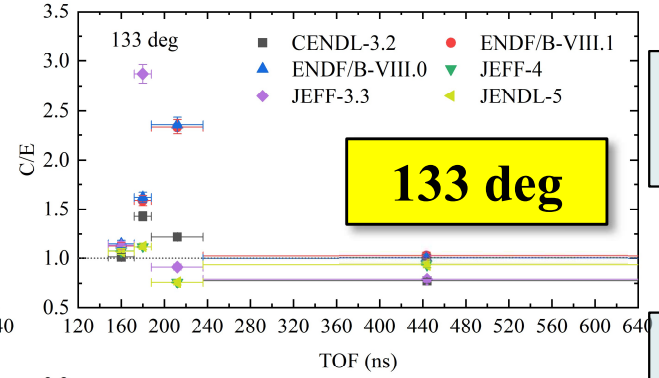

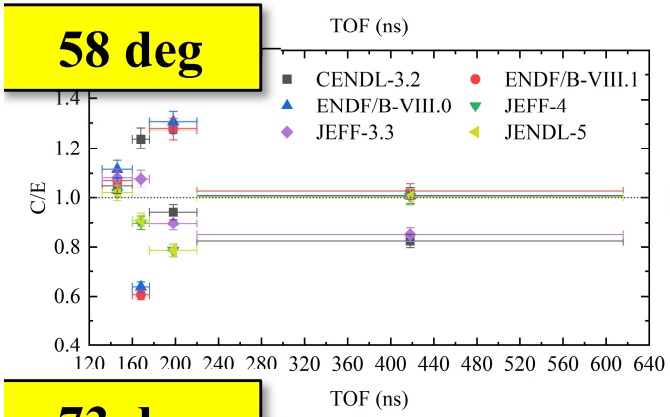

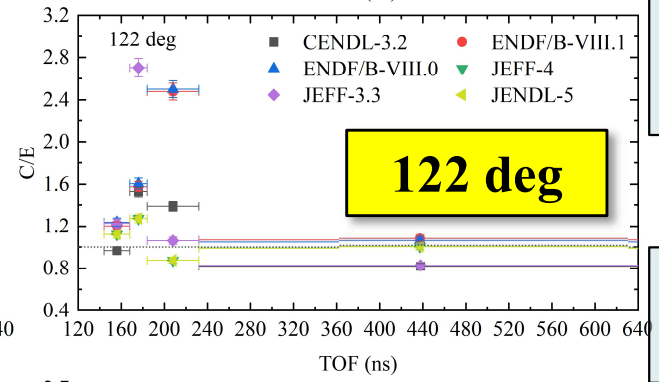

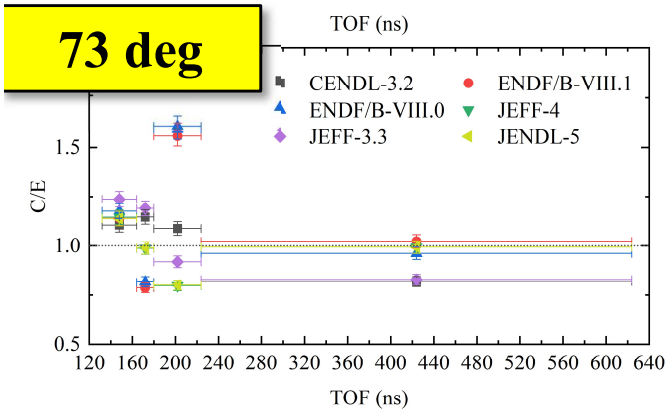

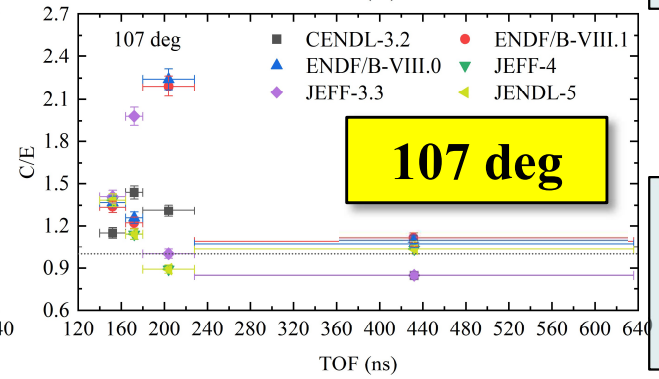

➢ **Elastic Region**

CENDL-3.2 shows the best overall agreement.

➢ **Discrete-Level Inelastic Region**

At **small angles JEFF-3.3** matches better, while at **large angles JENDL-5** is more accurate.

➢ **Continuous-Level Inelastic Region**

JEFF-3.3 performs best overall, and **CENDL-3.2** also performs well at **58°**

➢ **(n,2n) Region:**

CENDL-3.2 and **JEFF-3.3** significantly underestimate the results, while the others are generally close to **C/E ≈ 1**

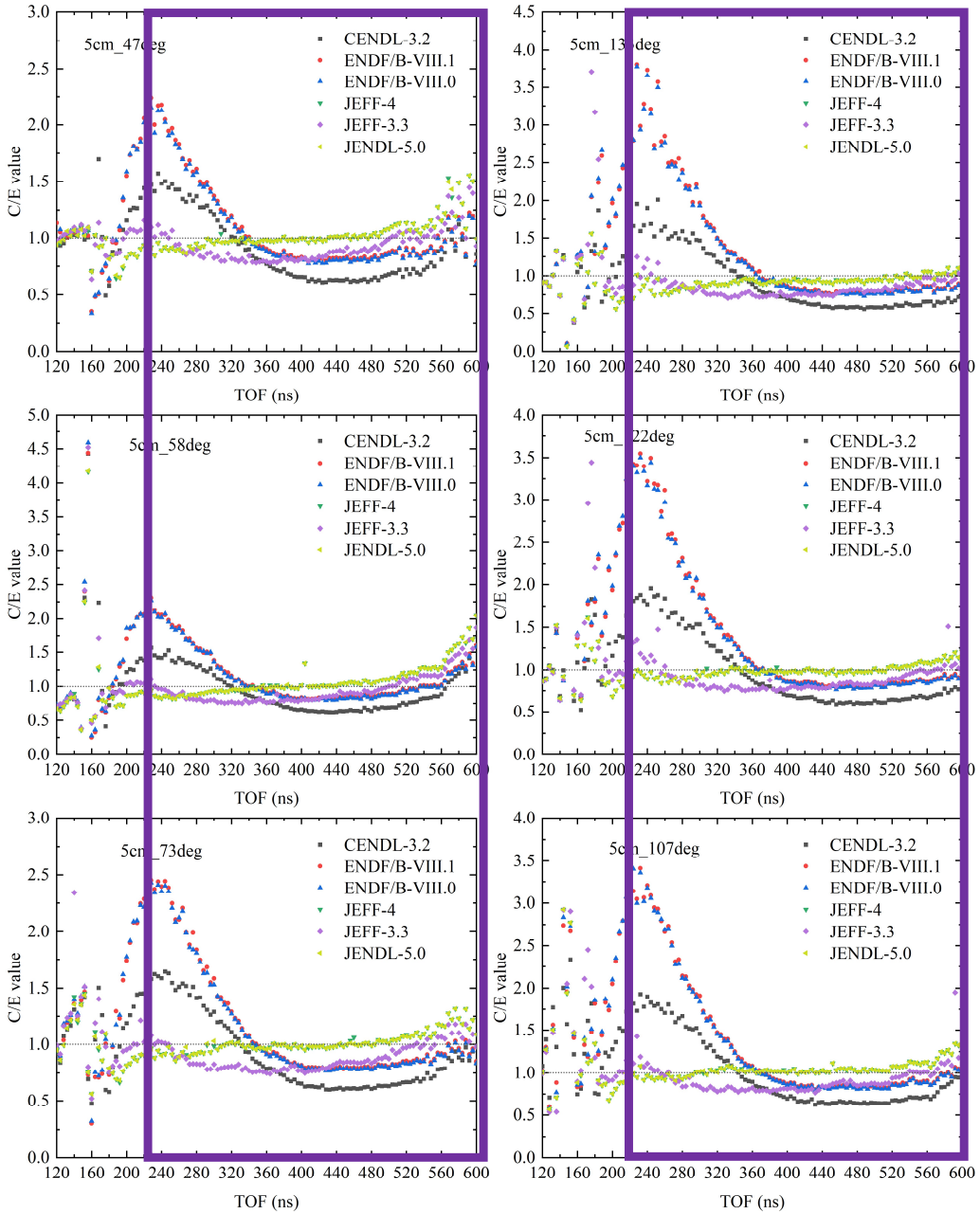

C/E values by each point for different nuclear data libraries at 5 cm thickness.

- **(n,2n) Region:**

ENDF/B-VIII.1, ENDF/B-VIII.0, JENDL-5, JEFF-4 all yield C/E values close to 1, but JENDL-5 and JEFF-4 show better spectral consistency, while ENDF/B-VIII.1 and ENDF/B-VIII.0 overestimate at high energies and underestimate at low energies.

Comparison of results across different nuclear data libraries.

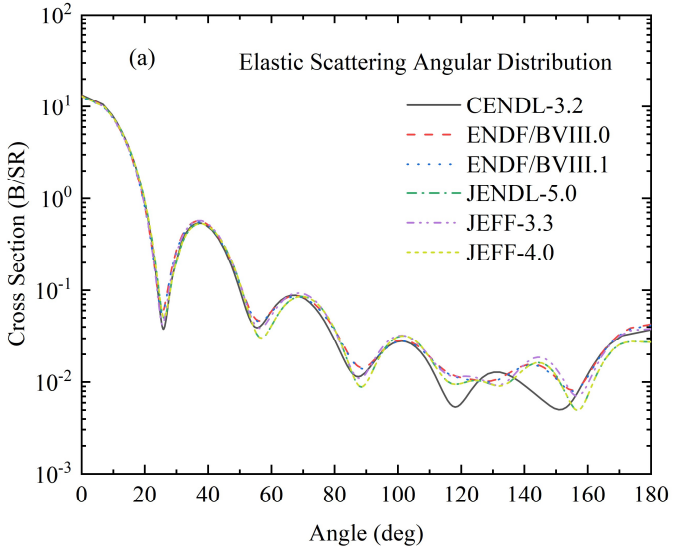

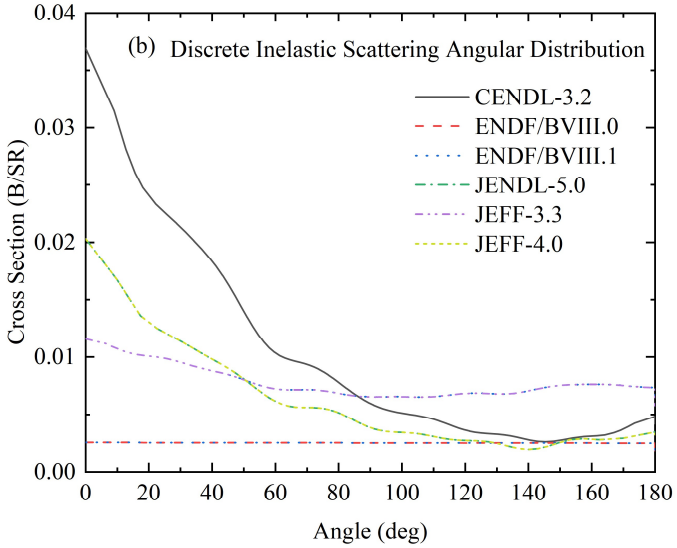

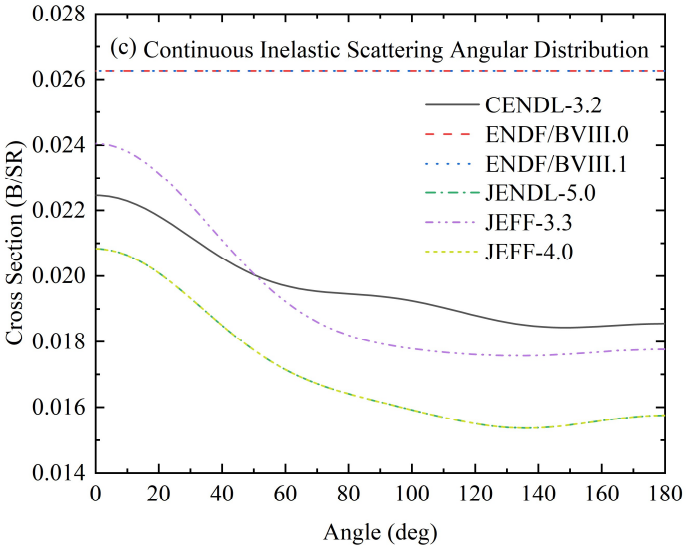

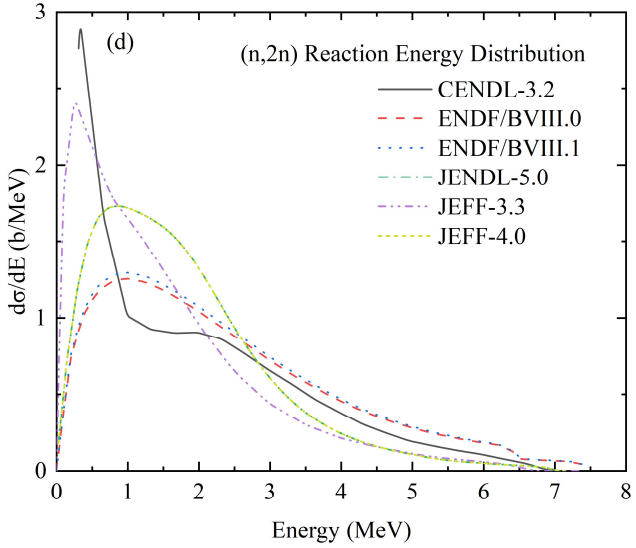

- **Elastic Region**

CENDL-3.2 provides best agreement across angles.

- **Discrete-Level Inelastic**

JENDL-5 is best at large angles; JEFF-3.3 performs well at small angles.

- **Continuous-Level Inelastic**

JEFF-3.3 is most accurate overall; CENDL-3.2 performs well at 58° .

- **(n,2n) Region:**

JENDL-5 is more consistent across the full range. **CENDL-3.2** and **JEFF-3.3** significantly underestimate the results.

Experimental Platform– Bi spherical Sample

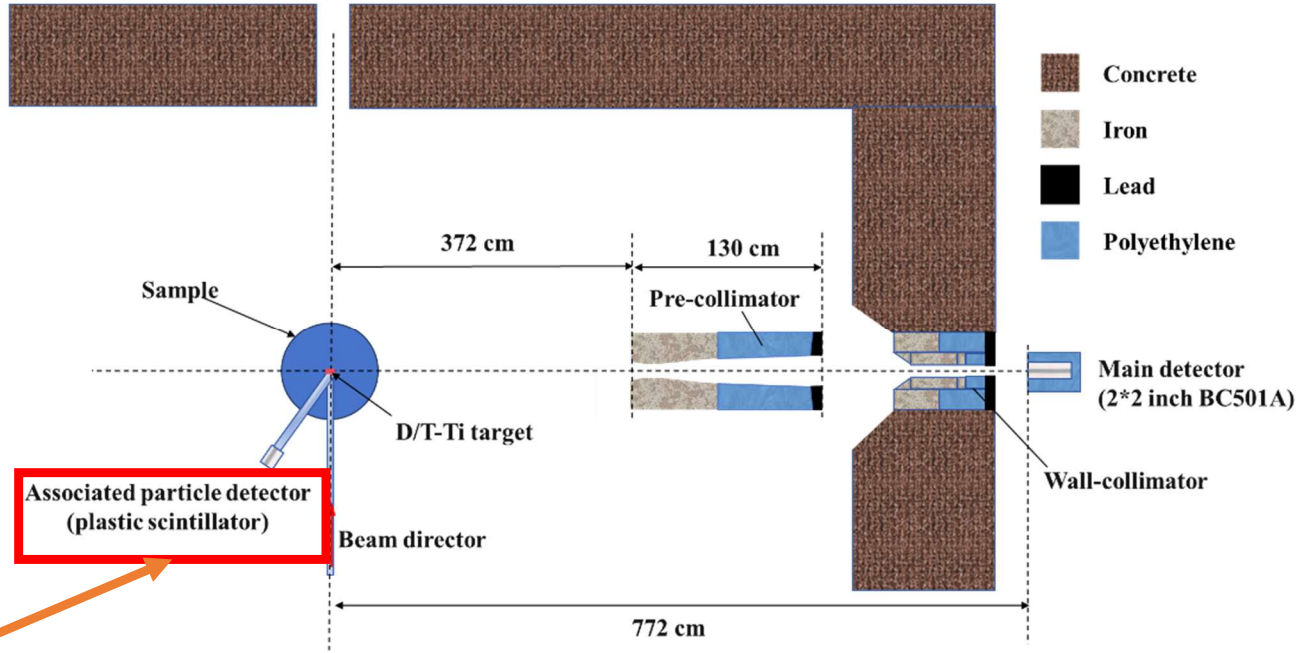

Because the sphere fully enclosed the target head and disabled the monitor system, the pulse time distribution was determined using the associated-particle detector.

Neutron leakage spectra were measured for three spherical Bi samples (diameters 19/29/39 cm, corresponding to penetration thicknesses of 5/10/15 cm).

The fast timing of the plastic scintillator enables time-of-flight (TOF) measurements of associated particles.
α particles and protons can be clearly separated in the measured spectrum.

Experimental characterization of the neutron source term: D–T/D–D mixed-field monitoring and pulse time distribution measurement.

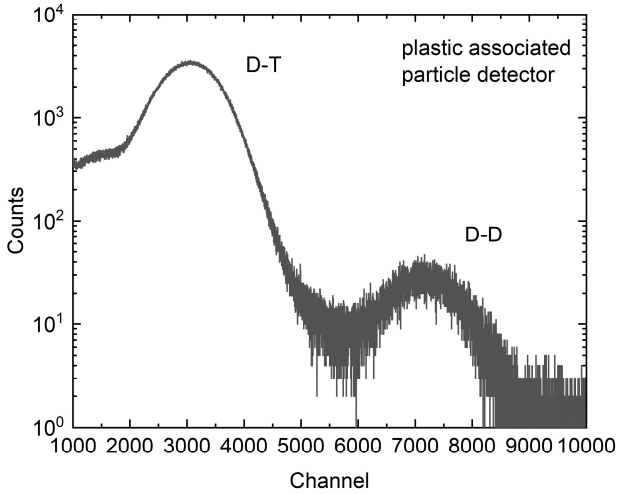

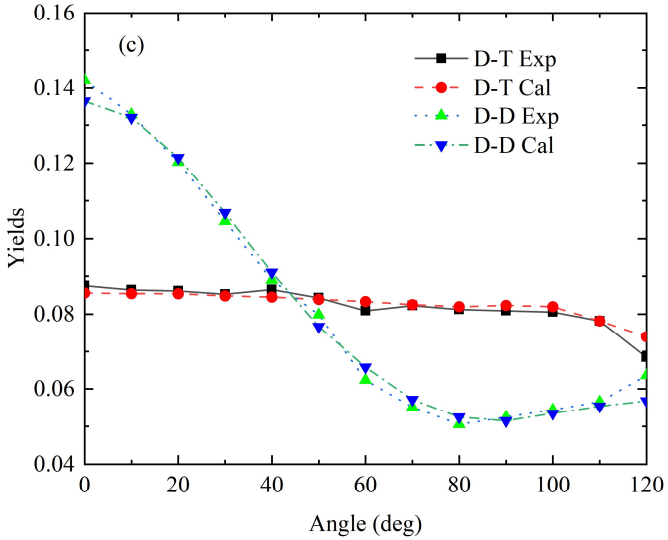

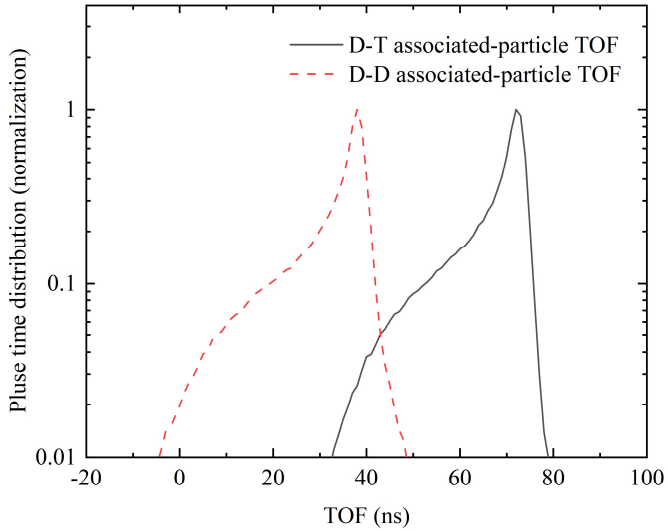

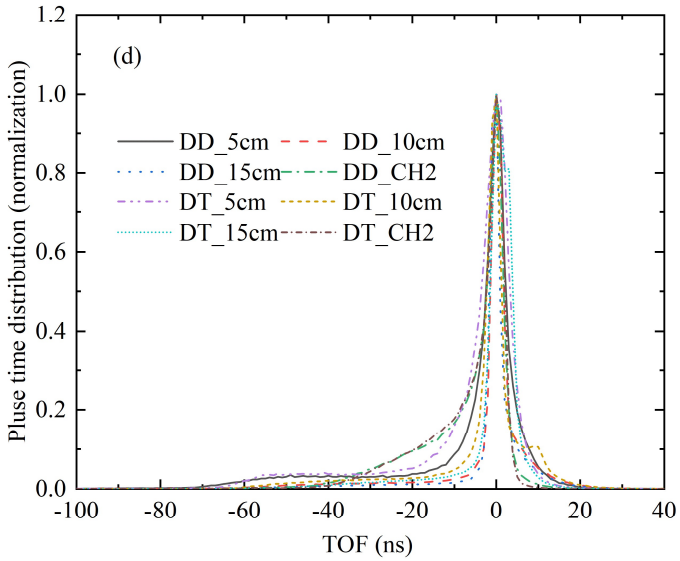

Experimental Results – Standard Sample (CH_2)

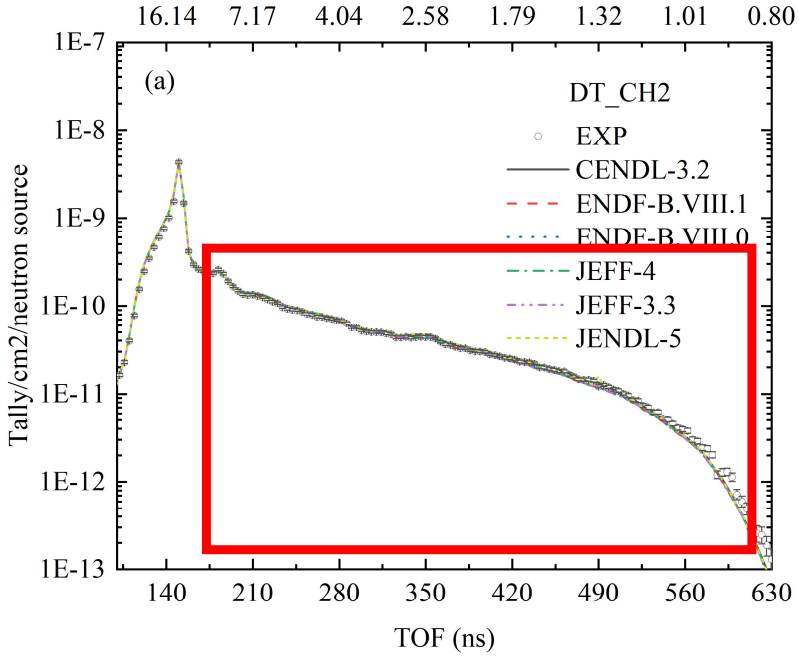

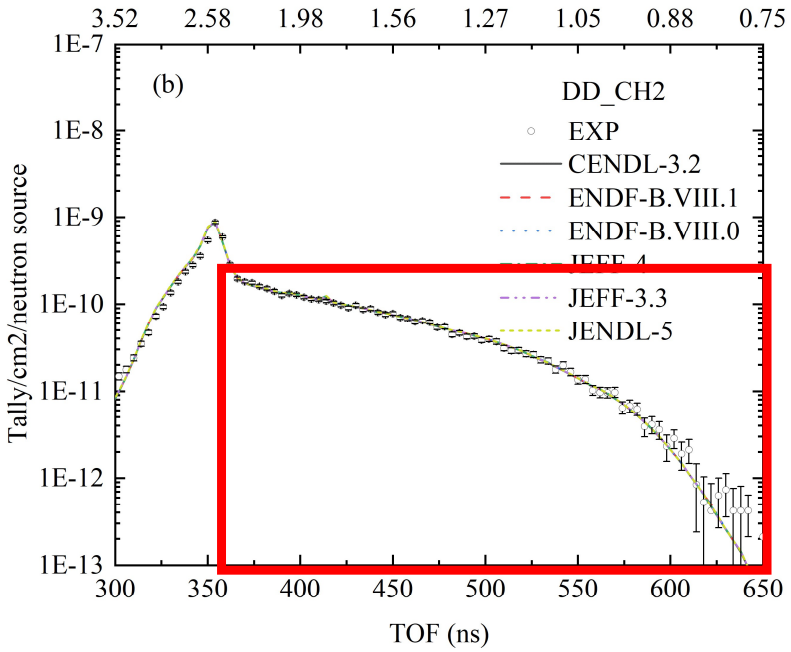

	CENDL-3.2	ENDF-B.VIII.0	ENDF-B.VIII.1	JENDL-5	JEFF-3.3	JEFF-4
			D-T_CH2			
experiment	5.892E-09	5.892E-09	5.892E-09	5.892E-09	5.892E-09	5.892E-09
calculation	6.007E-09	5.984E-09	5.984E-09	6.035E-09	5.980E-09	6.011E-09
C/E	1.019	1.016	1.016	1.024	1.015	1.020
			D-D_CH2			
experiment	3.730E-09	3.730E-09	3.730E-09	3.730E-09	3.730E-09	3.730E-09
calculation	3.738E-09	3.766E-09	3.766E-09	3.784E-09	3.760E-09	3.766E-09
C/E	1.002	1.010	1.010	1.014	1.008	1.010

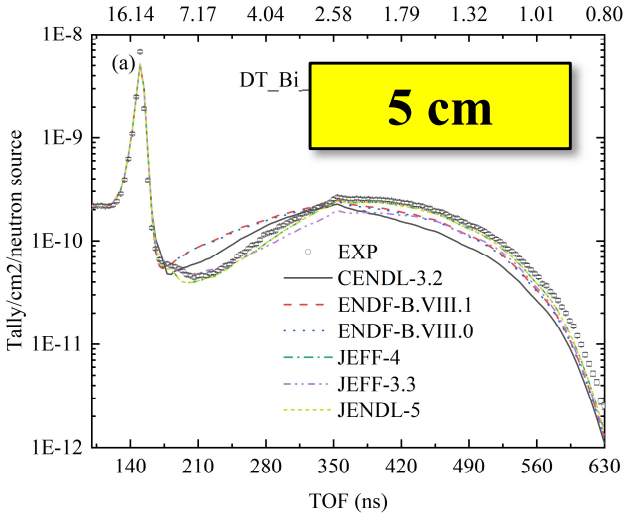

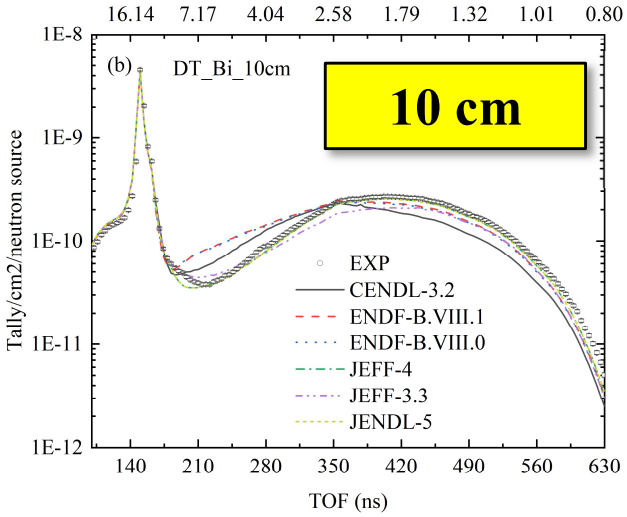

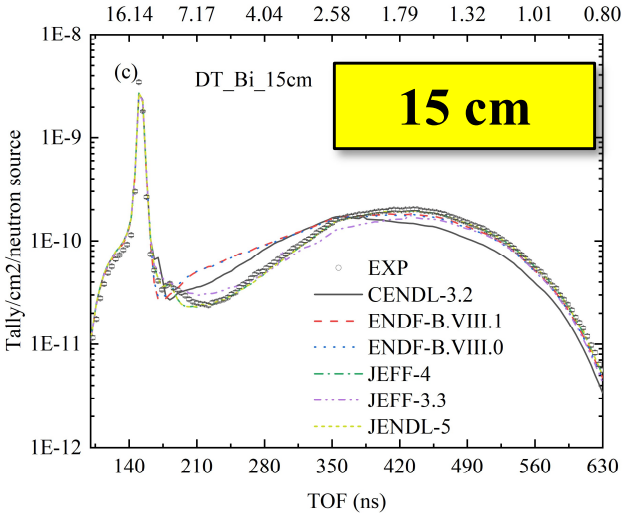

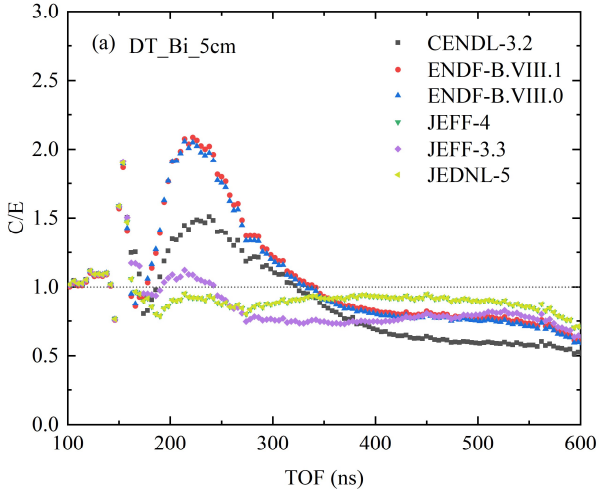

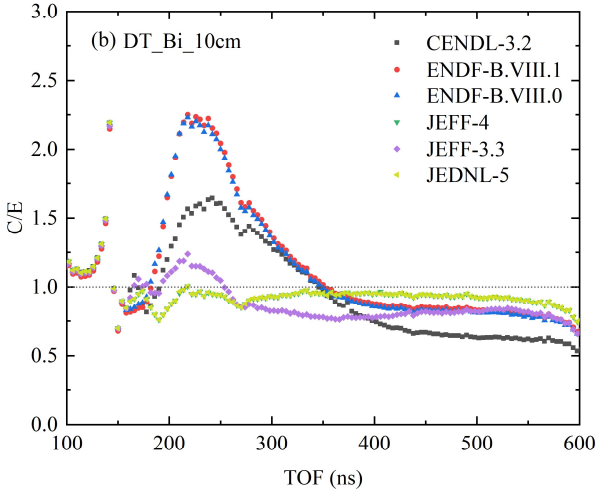

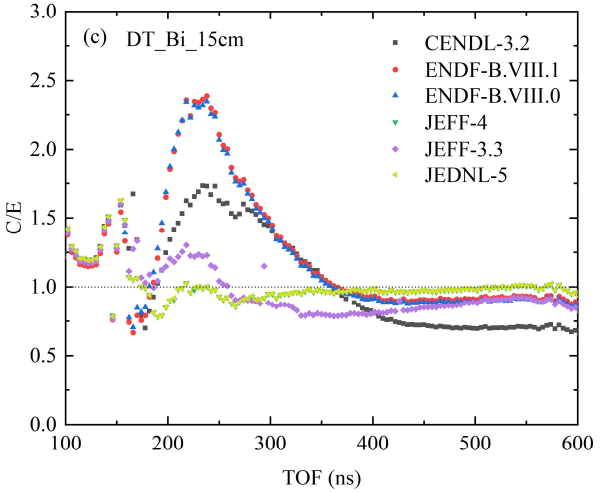

Experimental results at different thicknesses using a D–T neutron source, with point-by-point C/E comparisons against multiple nuclear data libraries.

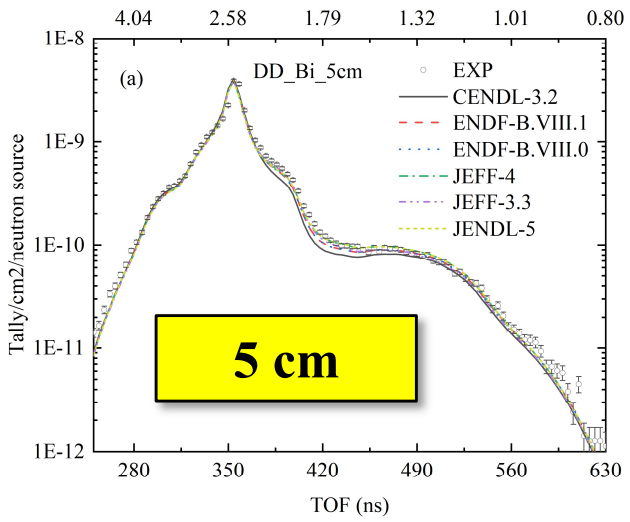

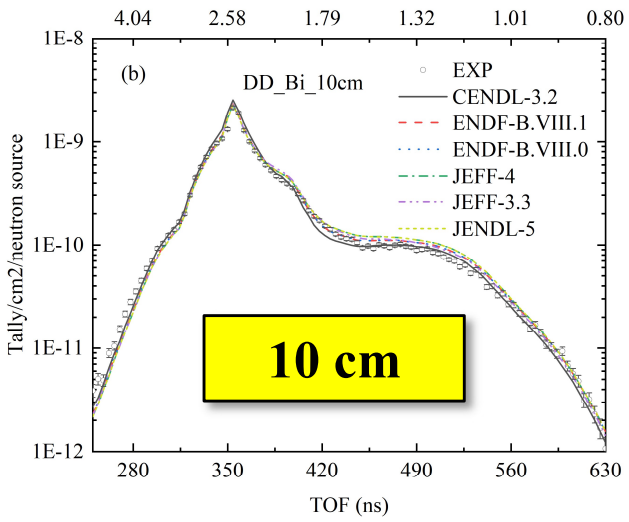

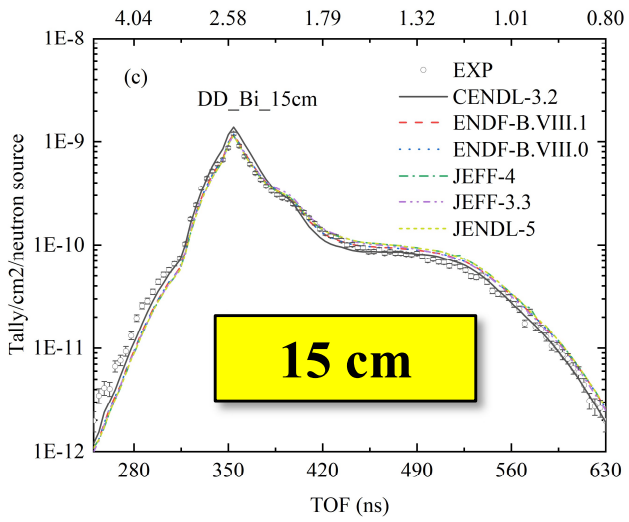

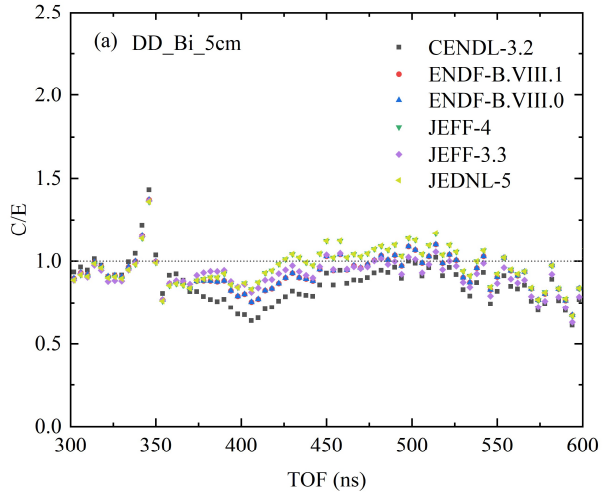

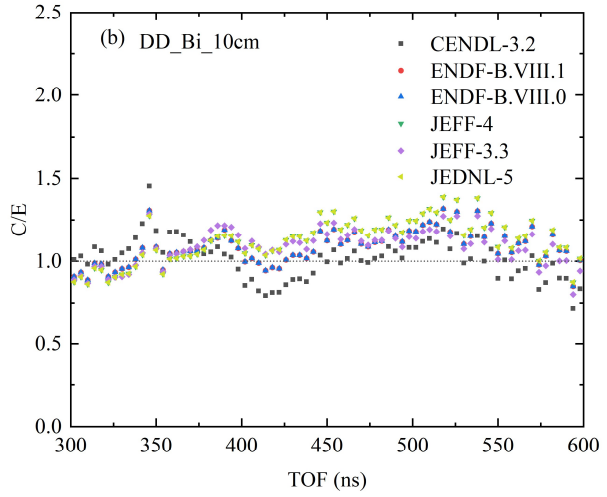

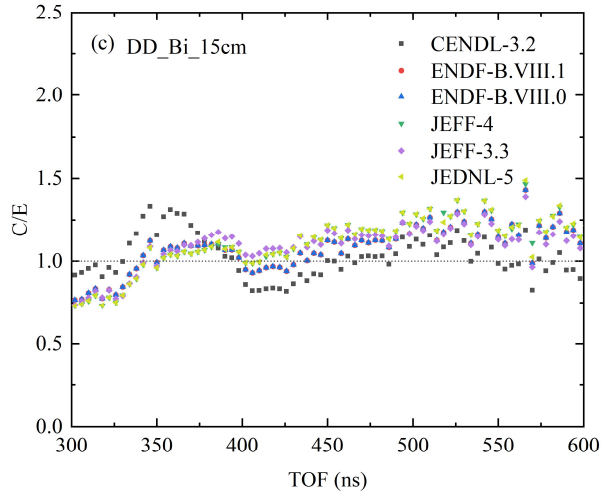

Experimental results at different thicknesses using a D–D neutron source, with point-by-point C/E comparisons against multiple nuclear data libraries.

➢ D-T neutron

The conclusions from the D–T source experiments are consistent with those from the slab-sample measurements.

➢ D-D neutron

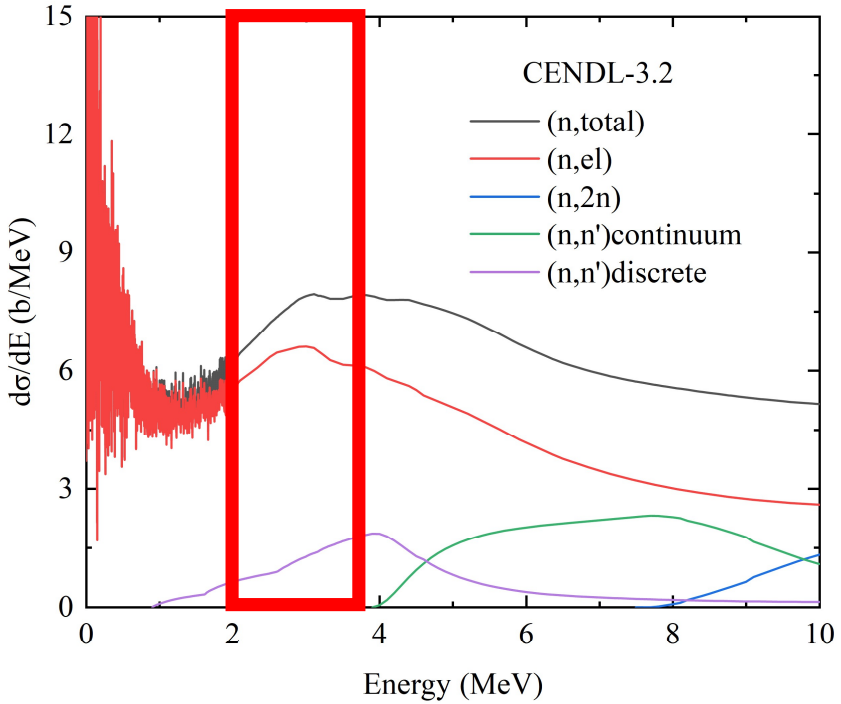

D-D neutron energy range

With a D–D neutron source, secondary neutrons mainly originate from elastic scattering and discrete-level inelastic scattering.

Reaction	Energy	TOF
(n,el)	>2.2MeV	<378ns
(n,n')discrete	0.8~2.2MeV	378~622ns

	CENDL-3.2	ENDF-B.VIII.0	ENDF-B.VIII.1	JENDL-5	JEFF-3.3	JEFF-4
			5cm			
(n,el)	0.991 ± 0.030	0.960 ± 0.029	0.960 ± 0.029	0.949 ± 0.029	0.954 ± 0.029	0.949 ± 0.029
(n,n')discrete	0.791 ± 0.024	0.894 ± 0.028	0.894 ± 0.028	0.947 ± 0.029	0.925 ± 0.028	0.947 ± 0.029
			10cm			
(n,el)	1.140 ± 0.035	1.034 ± 0.032	1.034 ± 0.032	1.004 ± 0.031	1.018 ± 0.031	1.004 ± 0.031
(n,n')discrete	0.989 ± 0.030	1.101 ± 0.034	1.101 ± 0.034	1.153 ± 0.035	1.145 ± 0.035	1.153 ± 0.035
			15cm			
(n,el)	1.178 ± 0.036	0.998 ± 0.031	0.998 ± 0.031	0.952 ± 0.029	0.973 ± 0.030	0.952 ± 0.029
(n,n')discrete	0.989 ± 0.030	1.077 ± 0.033	1.077 ± 0.033	1.124 ± 0.035	1.131 ± 0.035	1.125 ± 0.035

Comparison of results across different nuclear data libraries.

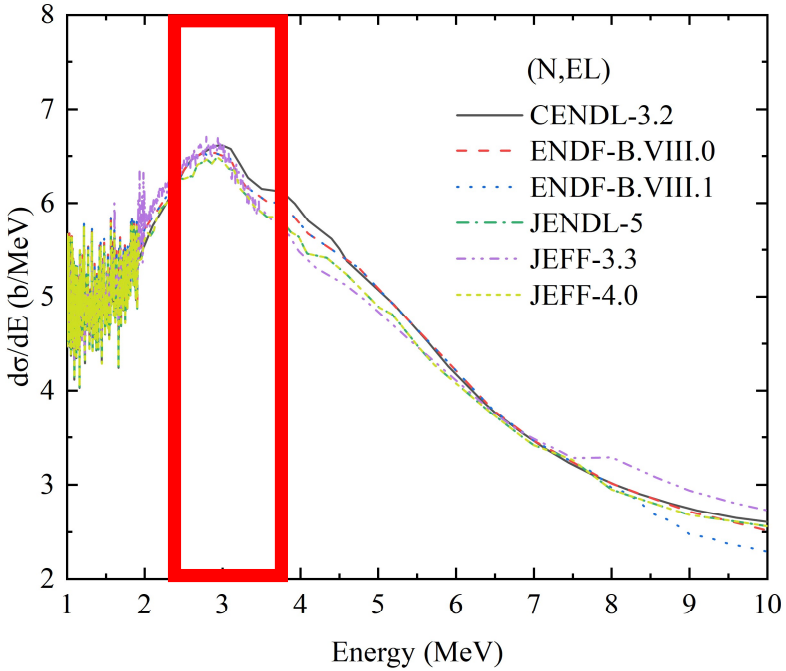

➢ **Elastic Region**

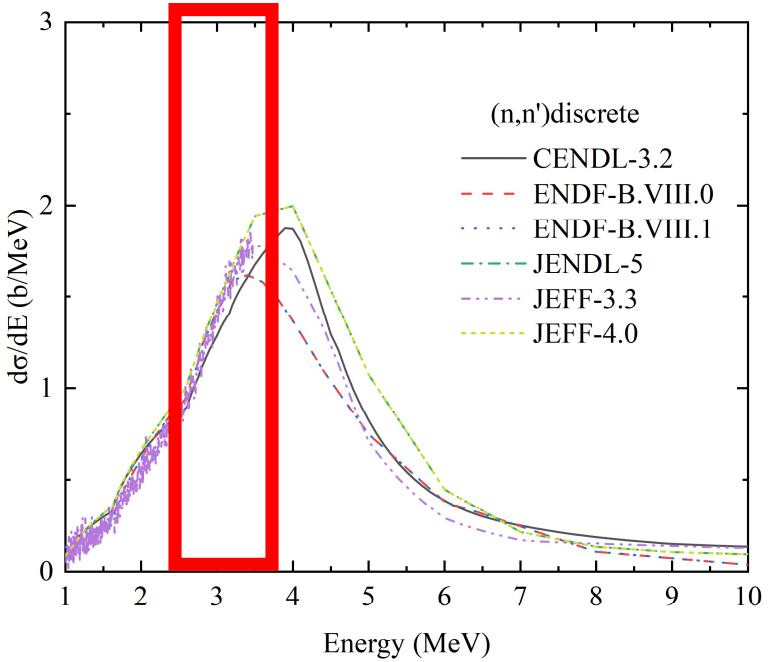

➢ **Discrete-Level Inelastic**

Overall, ENDF/B-VIII.1 and ENDF/B-VIII.0 provide the most accurate predictions; as thickness increases, CENDL-3.2 shows progressively higher C/E values.

CENDL-3.2 gives the lowest results among the libraries, while JENDL-5 and JEFF-4 tend to be higher; JENDL-5 and JEFF-4 performs better at 5 cm, whereas CENDL agrees better at 10 cm and 15 cm.

Spherical samples exhibit both leakage and reaction.

Comparison of results across different nuclear data libraries.

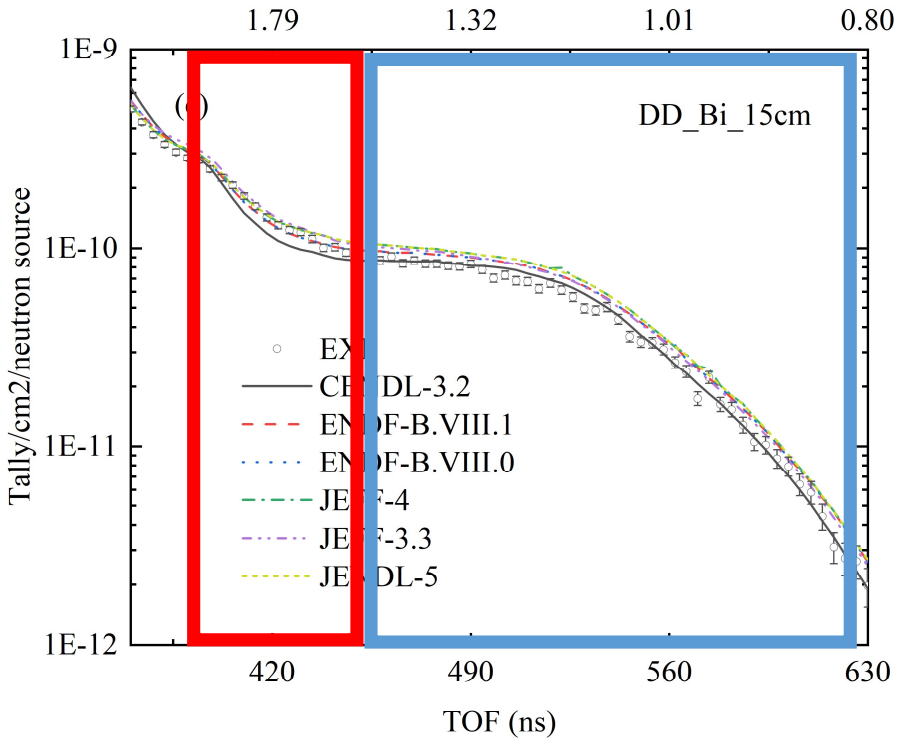

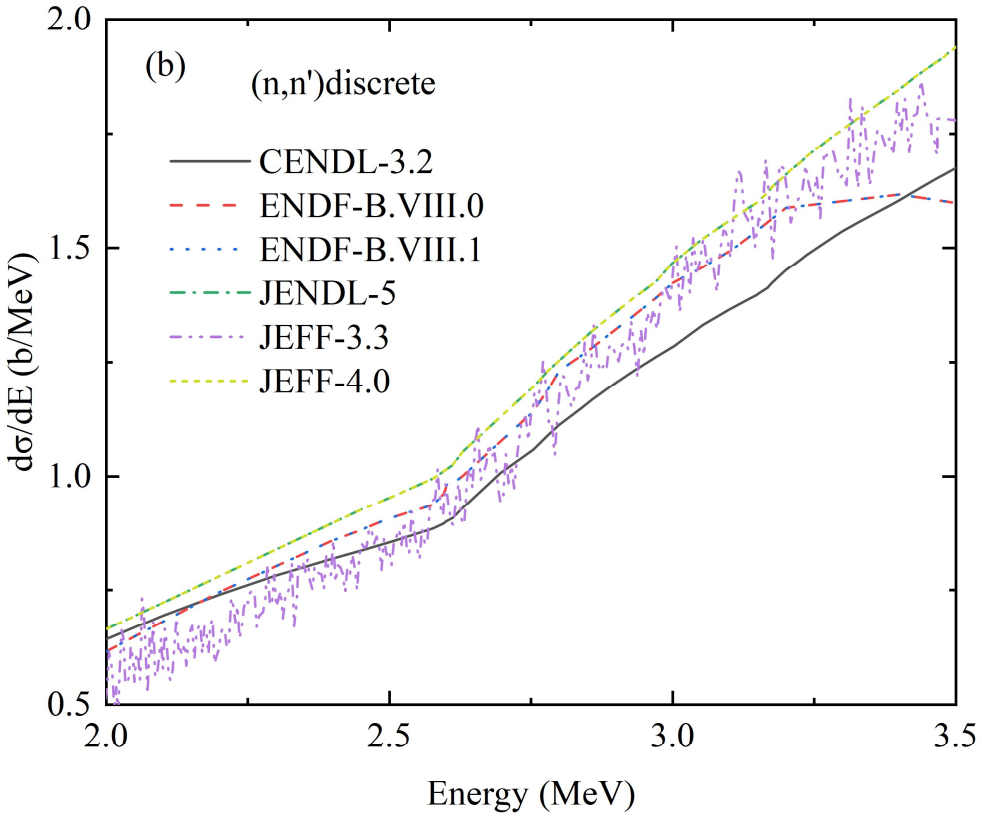

➢ **Discrete-Level Inelastic high energy**

CENDL shows a clear underestimation, while the other libraries give C/E values close to 1.

➢ **Discrete-Level Inelastic low energy**

CENDL shows the best agreement, while the other libraries tend to overestimate.

Experimental Platform– Cf-252 neutron source

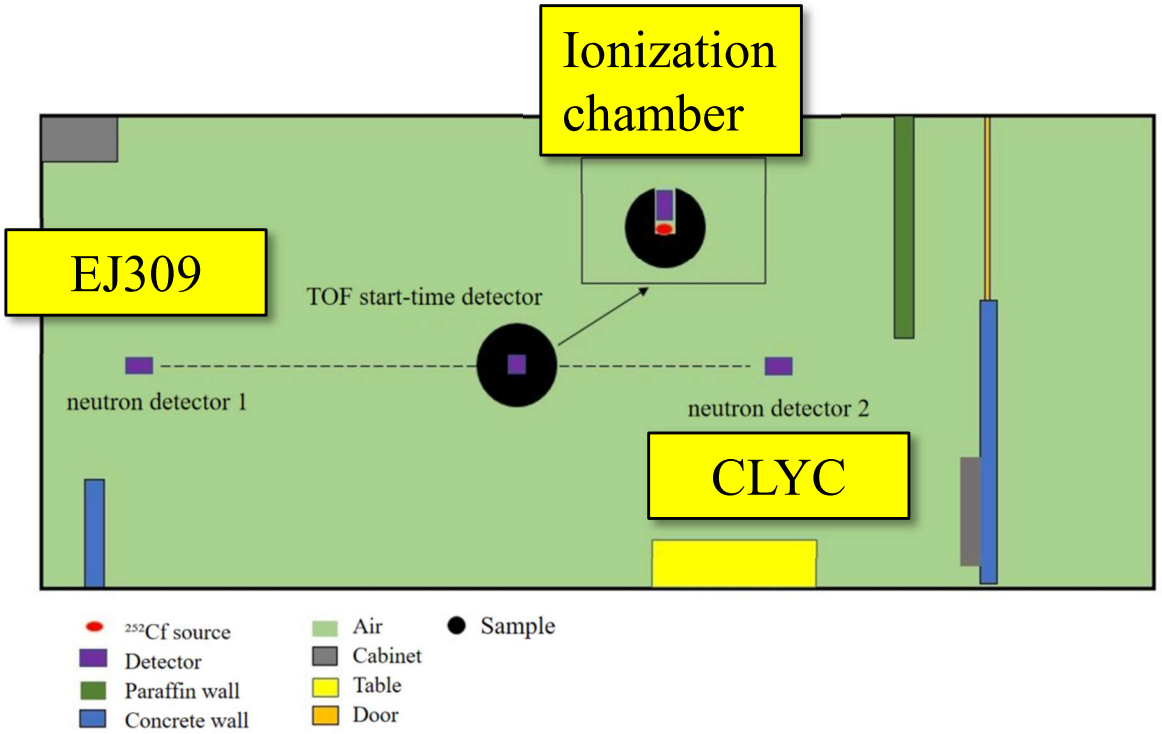

Diameters=2.9cm

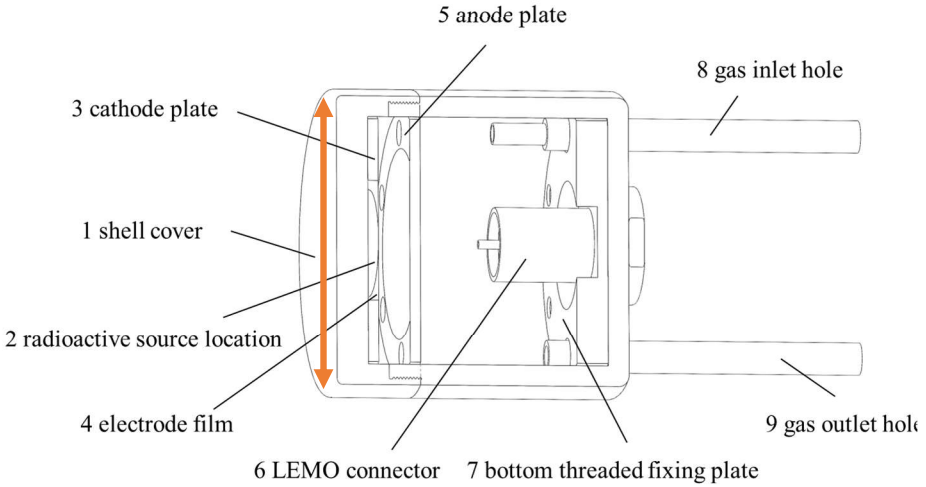

Cf-252:
Stable, near-isotropic point-like emission simplifies geometry modeling and uncertainty control.
A representative fission neutron spectrum (~2 MeV mean energy) is well suited for validating shielding attenuation and spectral shaping.

Cs_2LiYCl_6 :Ce(CLYC) Detector

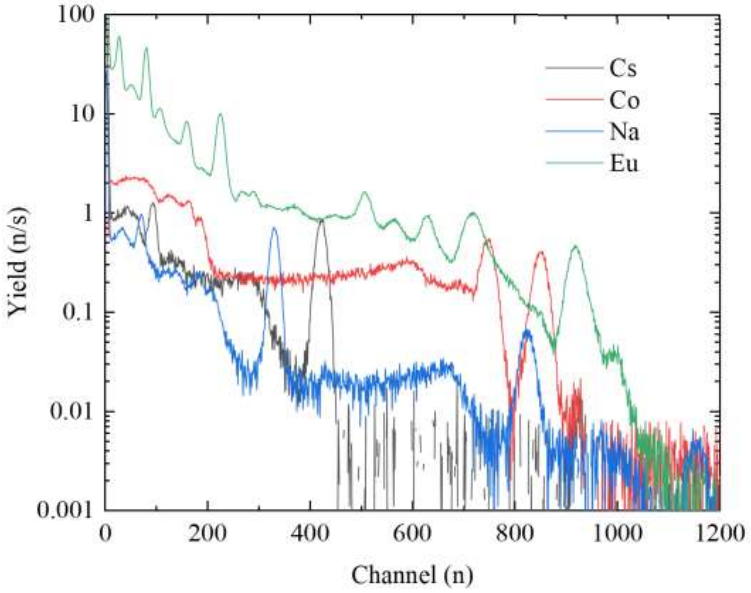

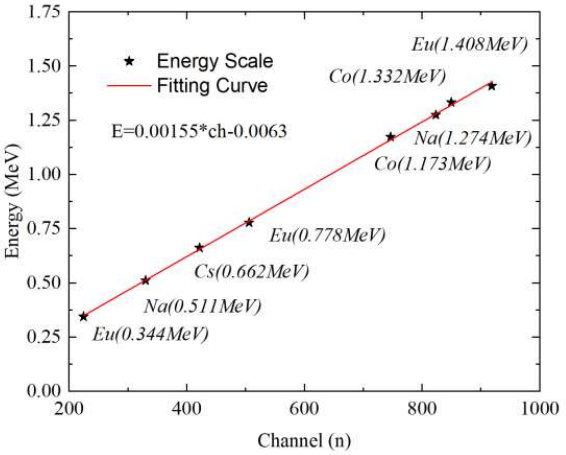

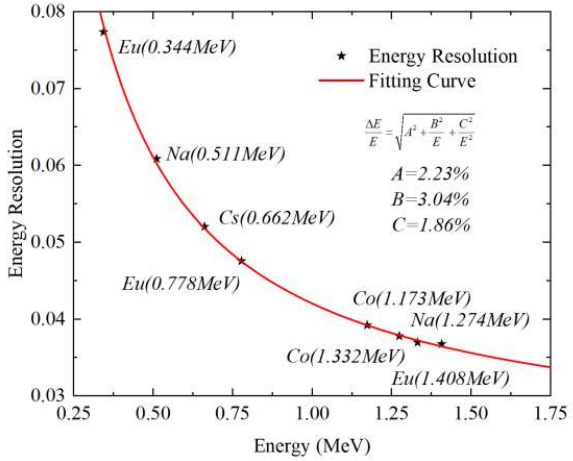

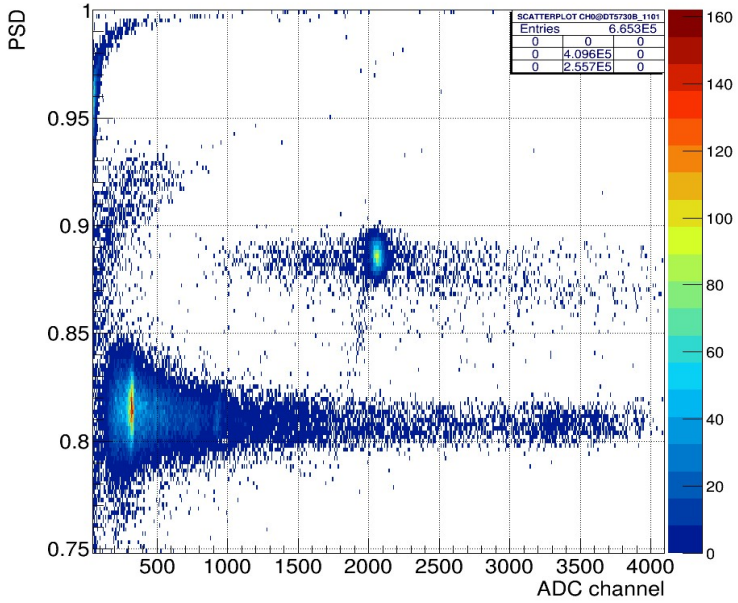

Li doping enables low-energy neutron detection, while chlorine (Cl) doping provides fast-neutron sensitivity via the $^{35}Cl(n,p)$ reaction.

Excellent n–γ discrimination, with a typical FOM > 2.

Gamma-ray energy resolution is ~5% at 662 keV.

Experimental Results – Standard Sample (CH_2)

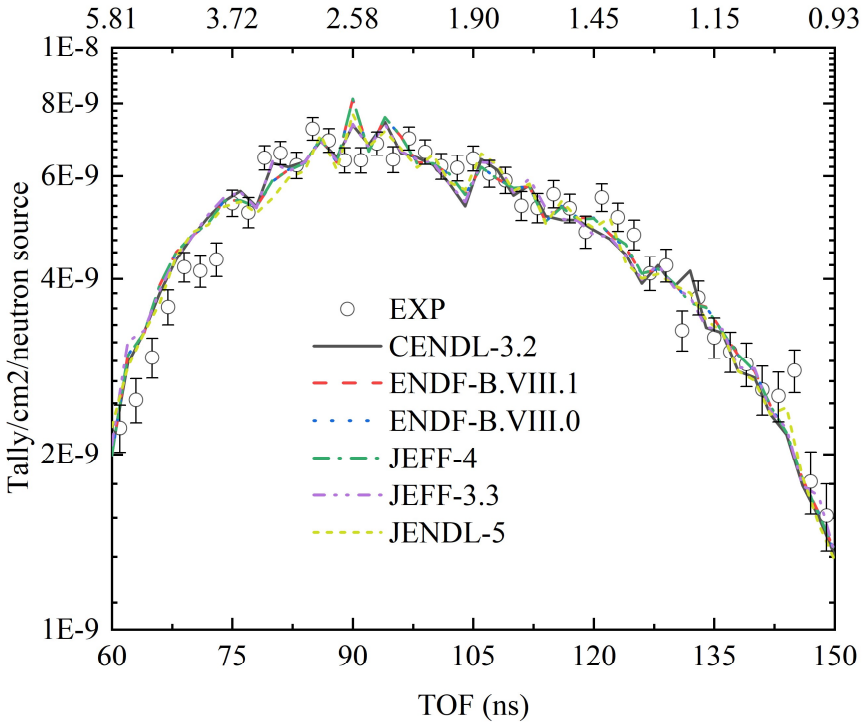

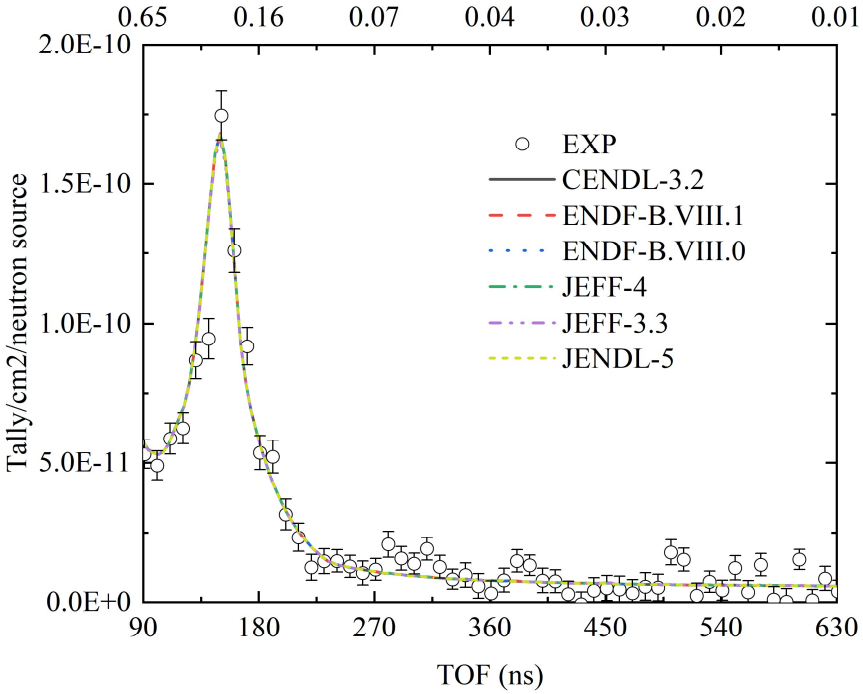

A 12 cm-diameter polyethylene sphere was used as the benchmark sample to validate the platform, with C/E deviations < 5% across libraries.

Experiments with two Fe samples (12 cm and 24 cm in diameter) have been completed.

Experiments are underway for three Bi samples (10/15/20 cm in diameter).

Quasi-Differential Neutron Scattering experiment platfor
CSNS Back-n

China's pulsed spallation neutron source uses 1.6 GeV proton pulses (25 Hz) striking a tungsten (W) target to generate intense pulsed neutrons.

CSNS currently operates at ~170 kW beam power.

CSNS typically operates with two proton bunches per pulse separated by ~410 ns, which boosts intensity/neutron flux (single-bunch gives about half the flux)

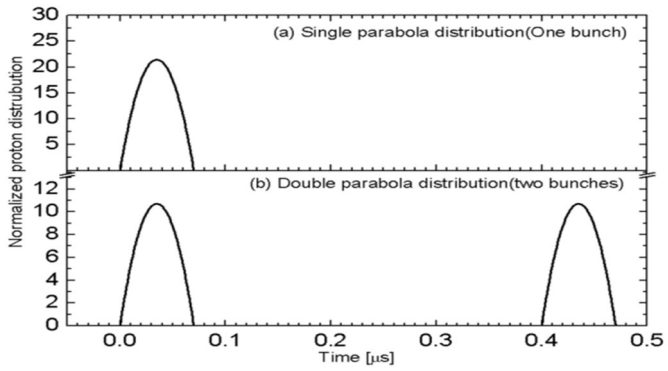

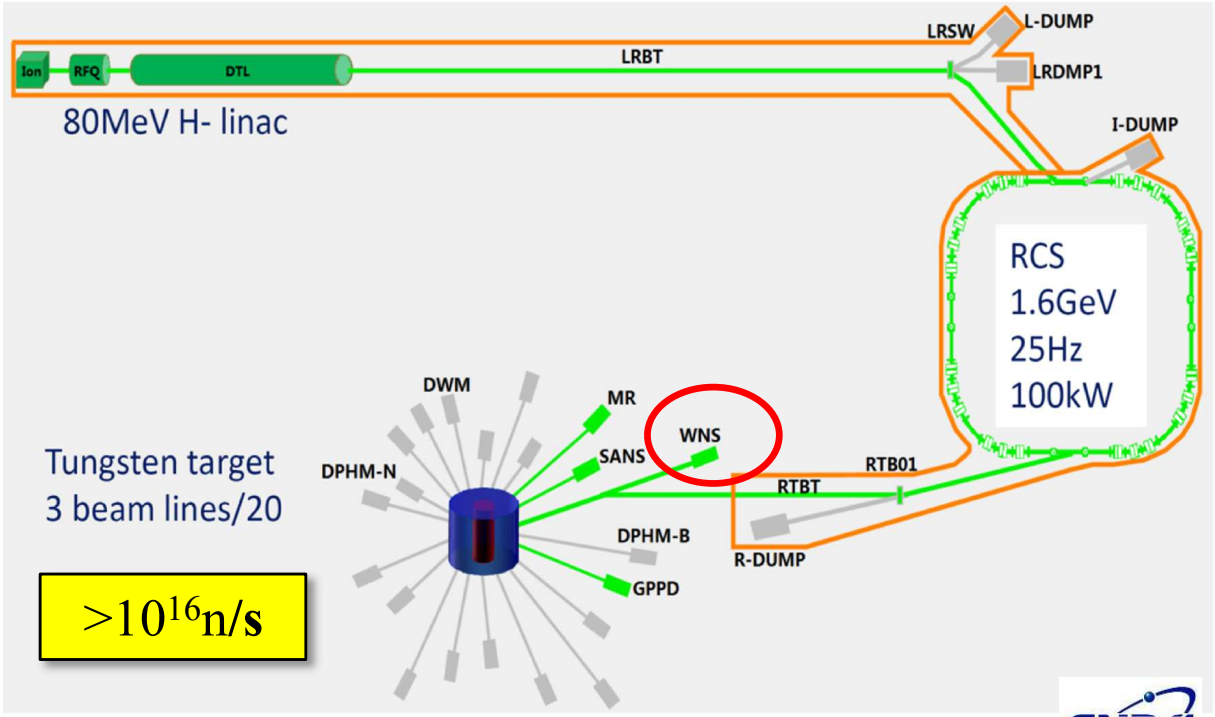

Beam spot size and energy spectra under different shutter configurations.

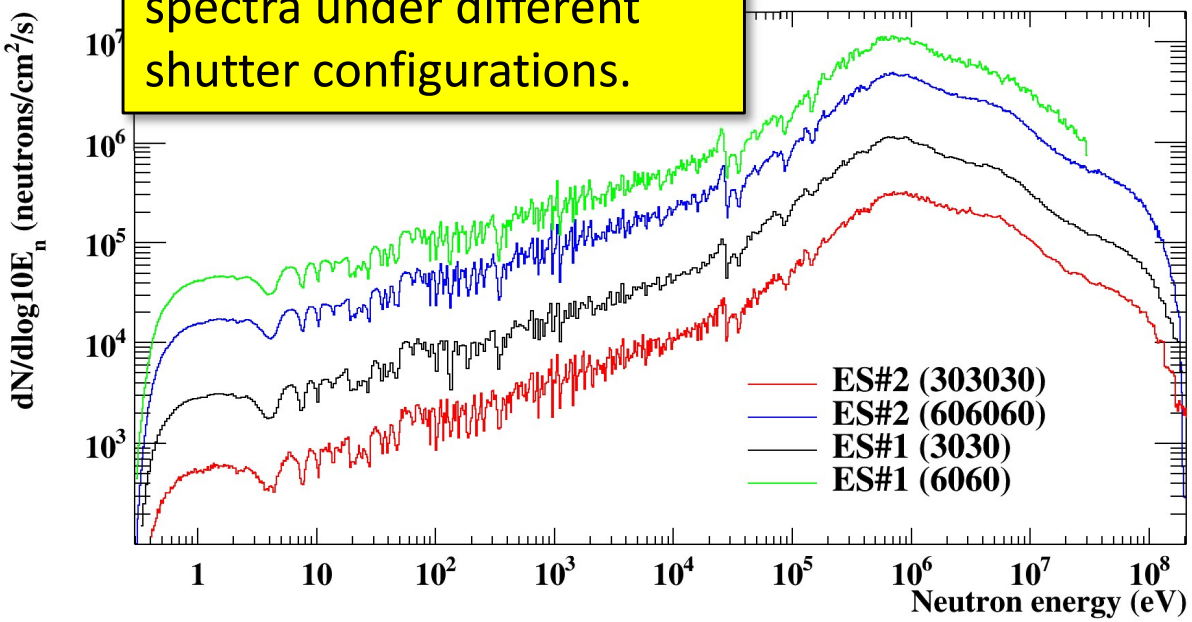

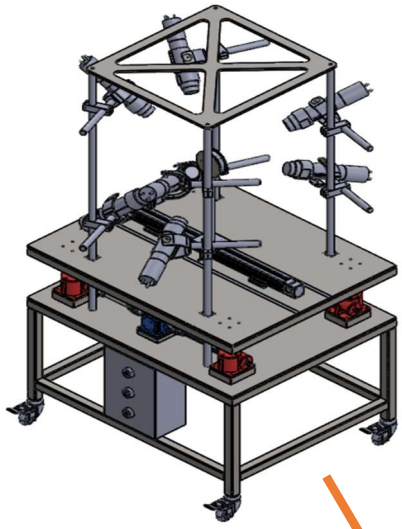

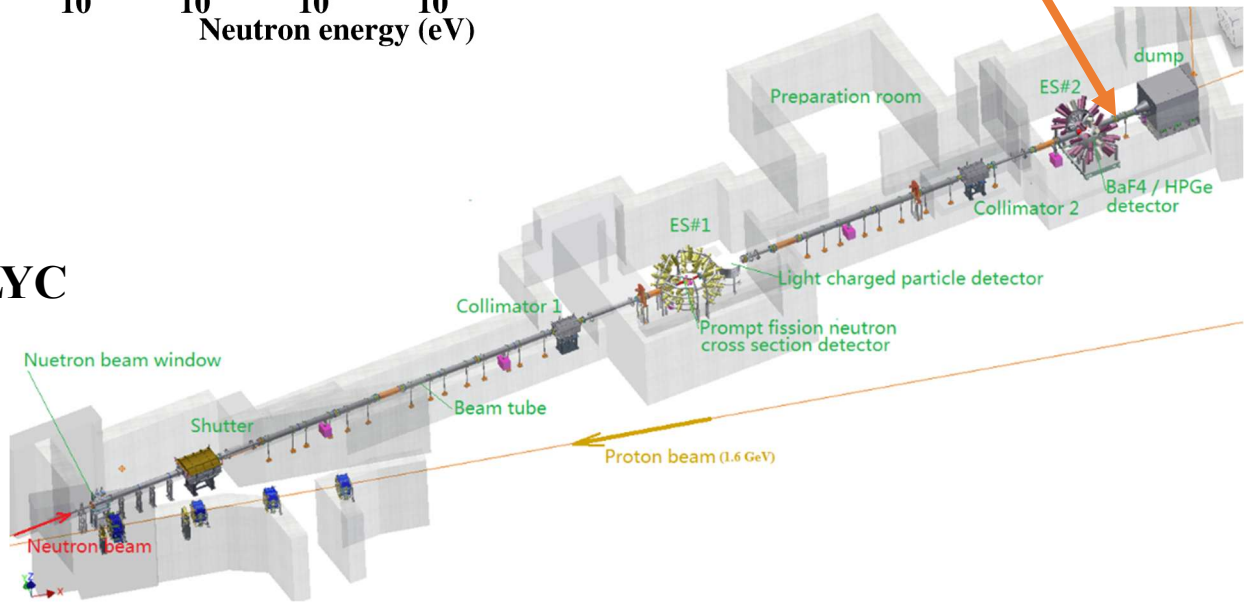

- **Location: Hall 2**
- **Beam power: 160 kW**
- **beam spot: Ø30 mm**
- **Detectors: 4 × BC501A + 4 × CLYC**
- **Samples: 20 mm Graphite, Zr**
- **Distances: source–sample 77.4 m;**
- **sample–detector 0.3 m**
- **Angles: 30°, 70°, 110°, 150°**
- **DAQ system: XIA**

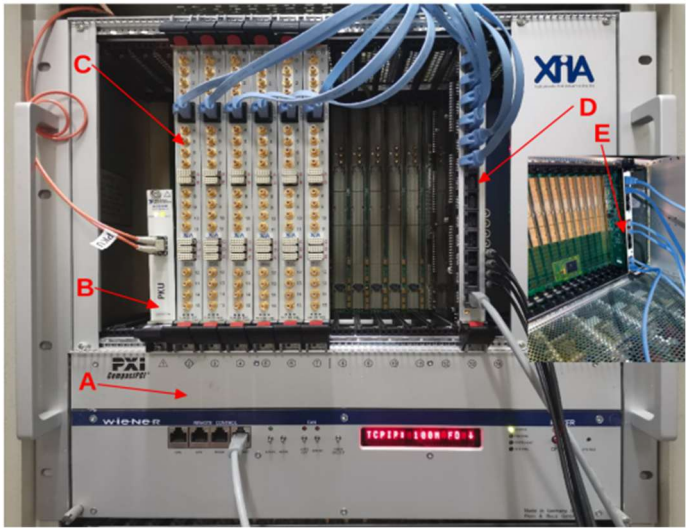
C
D
E
B
A
XHA
PXI
wiener

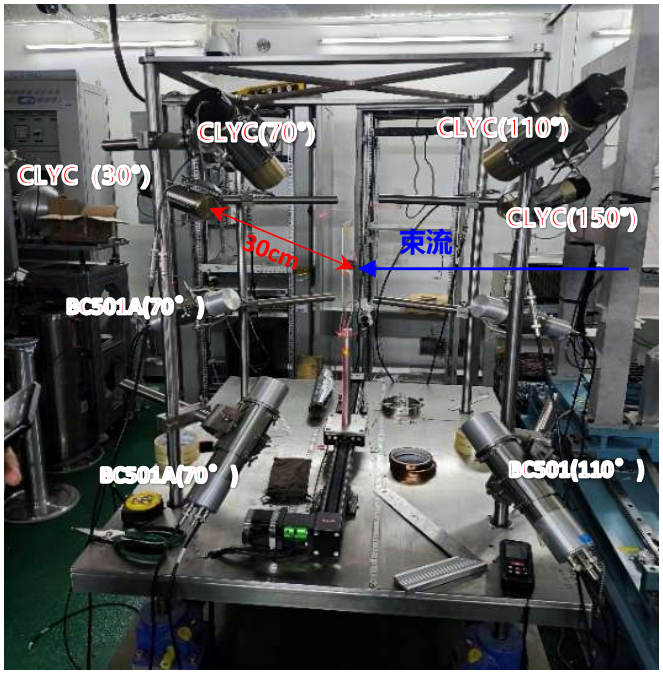
CLYC(70°)
CLYC(110°)
CLYC（30°）
CLYC(150°)
30cm
束流
BC501A(70°)
BC501A(70°)
BC501(110°)

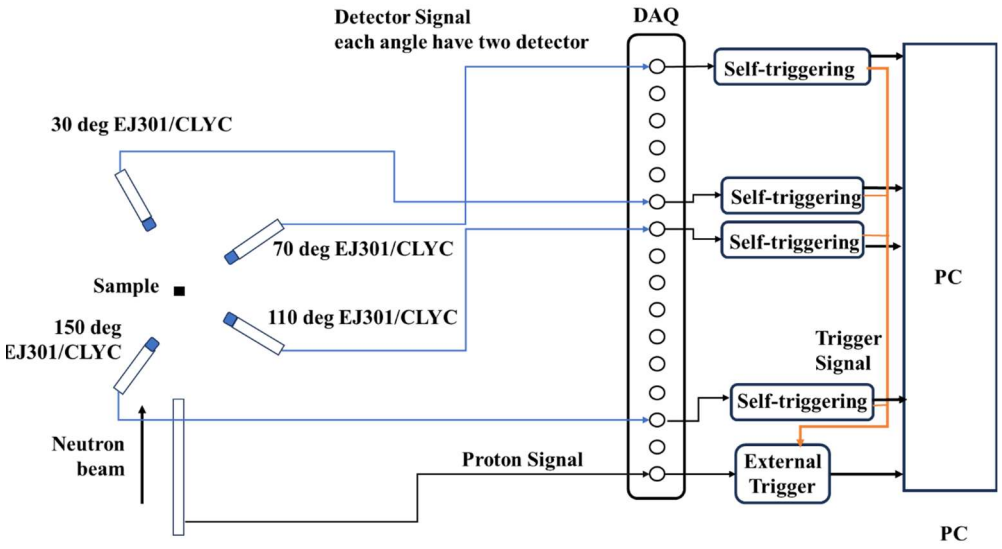
Detector Signal
each angle have two detector
DAQ
30 deg EJ301/CLYC
70 deg EJ301/CLYC
Sample
110 deg EJ301/CLYC
150 deg
EJ301/CLYC
Neutron
beam
Proton Signal
Self-triggering
Self-triggering
Self-triggering
Trigger
Signal
Self-triggering
External
Trigger
PC
PC


C
Zr
Zr
Zr

IAEA NEUTRON DATA STANDARDS (2017)

5 ^{nat}C(n,n) up to 6.45 MeV
(Standard range: 1keV - 1.8 MeV, angular distribution standard)

Detector Energy Range:
BC501A >0.8MeV
CLYC 0.03MeV~1.2MeV

Double-beam analysis:
A MLEM-based unfolding algorithm

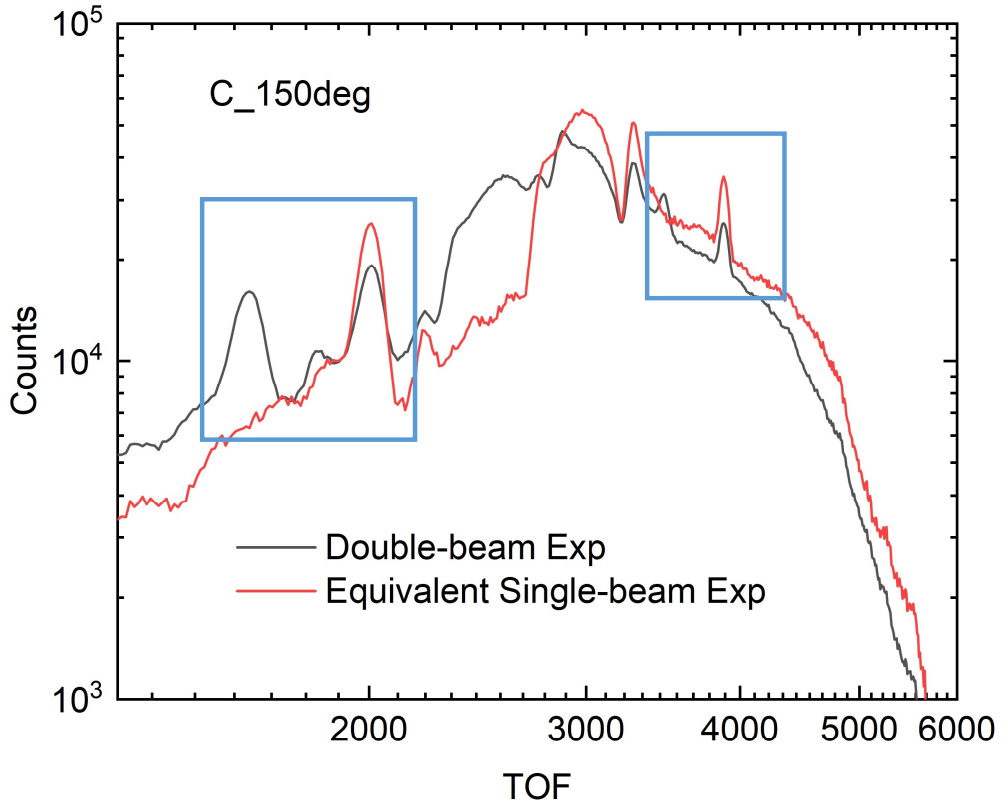

Experimental Results – Standard Sample (C) – CLYC

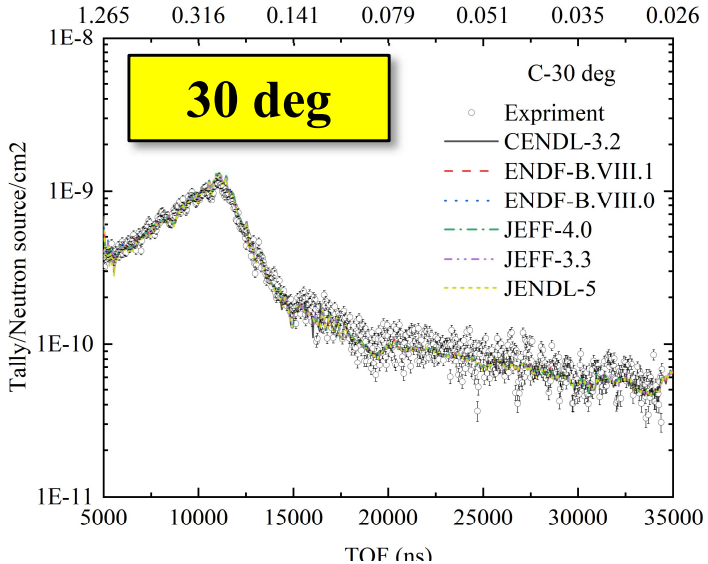

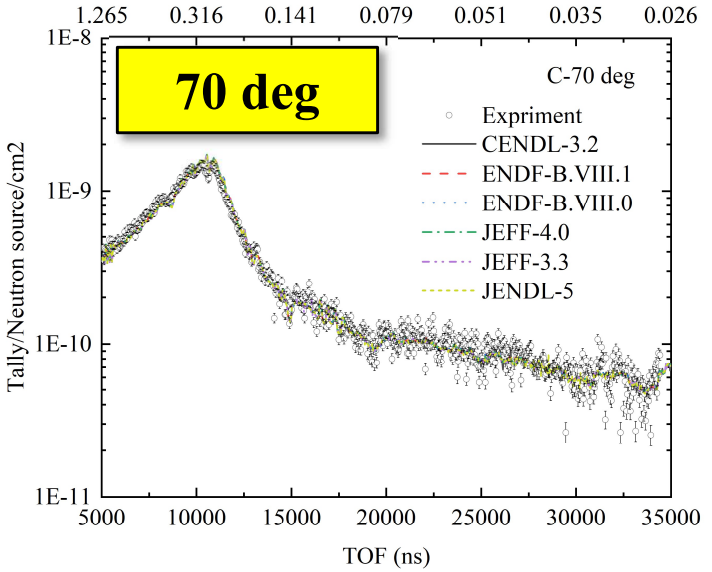

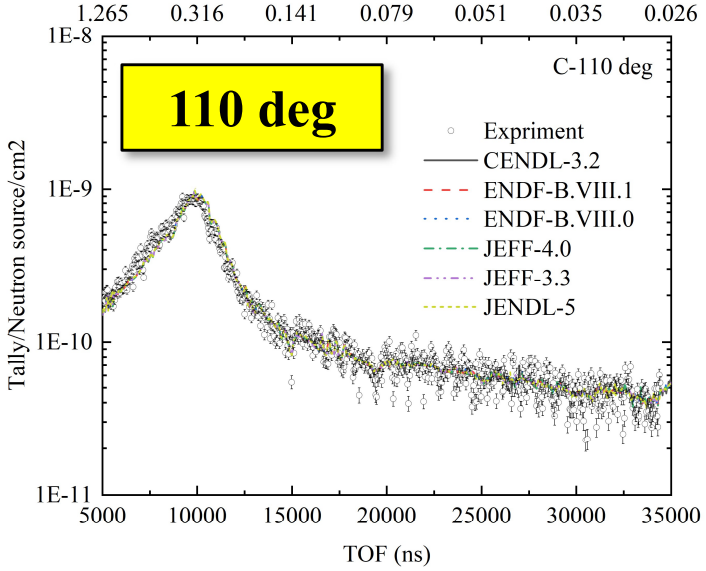

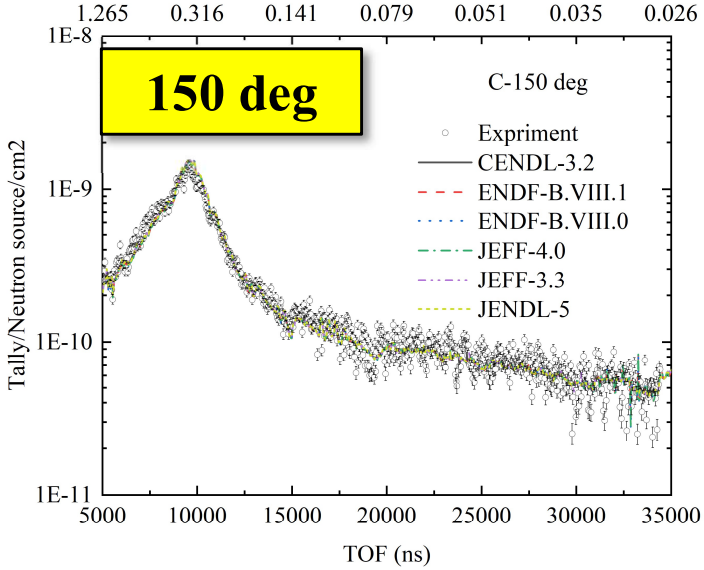

The C/E values across all databases and perspectives are close to 1.

Experimental Results – Standard Sample (C) – BC501A

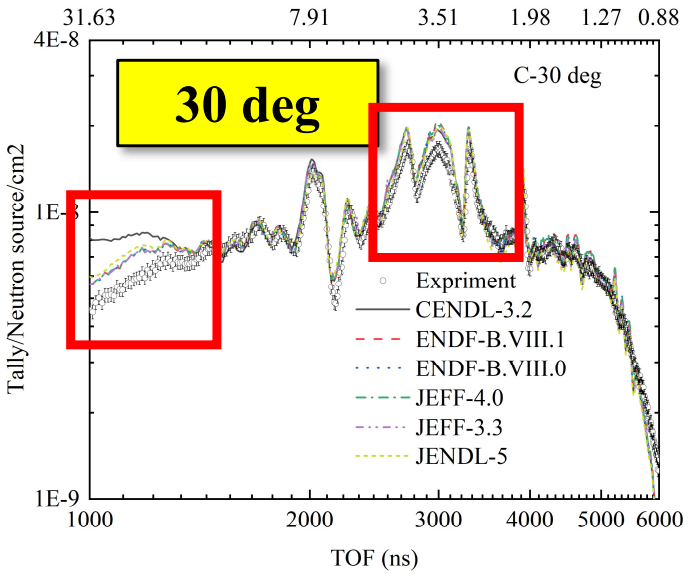

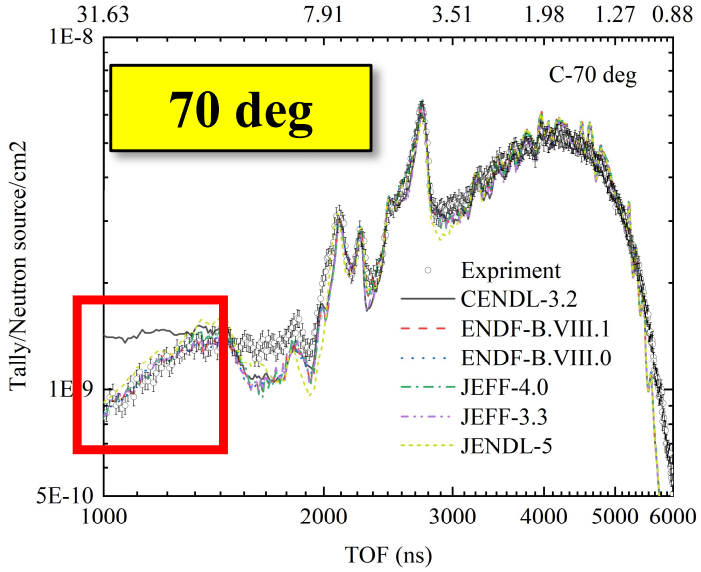

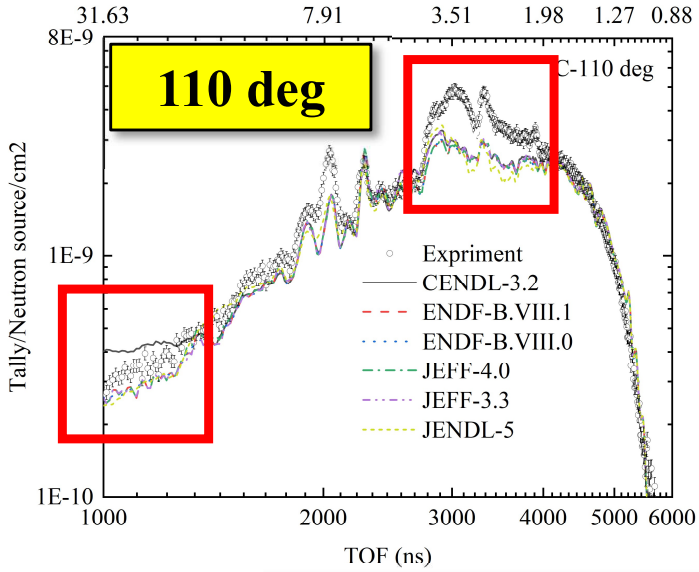

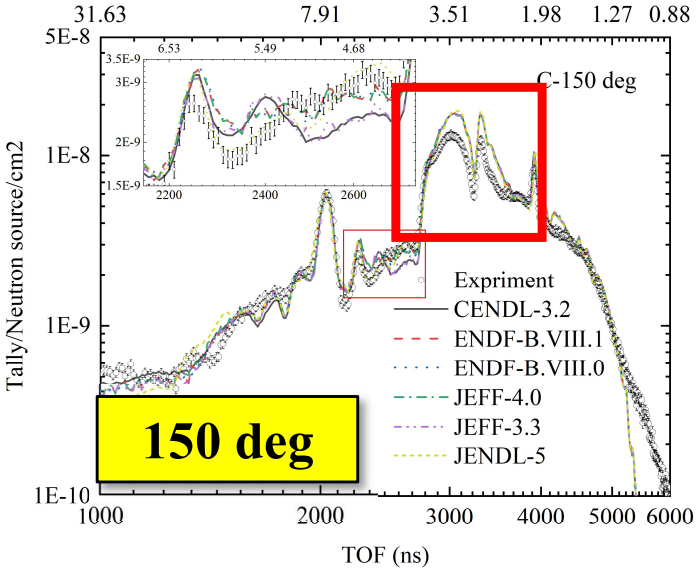

Energy Range:
<6.45MeV
Stander cross-section but not stander angular distribution

6.45MeV~20MeV

>20MeV

The angular distribution of C in the fast neutron energy region still exhibits significant deviation.

<6.45MeV

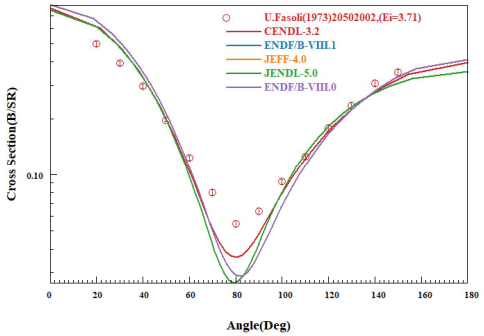

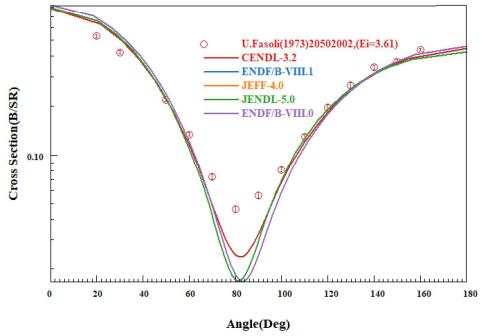

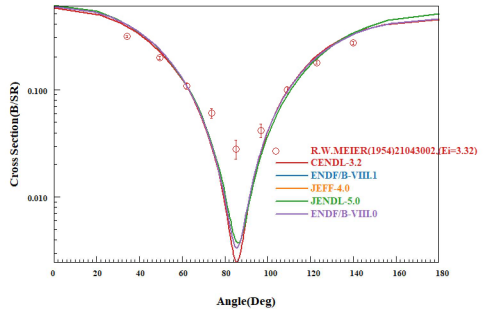

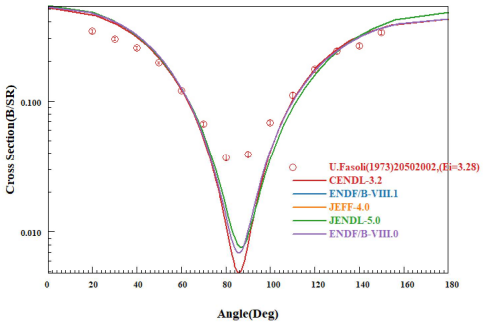

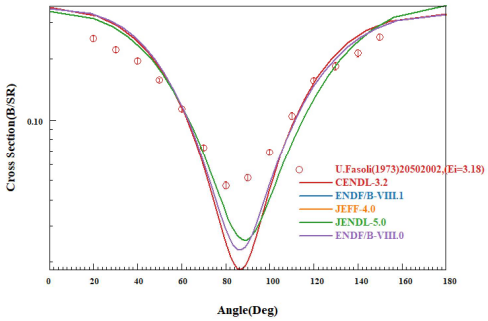

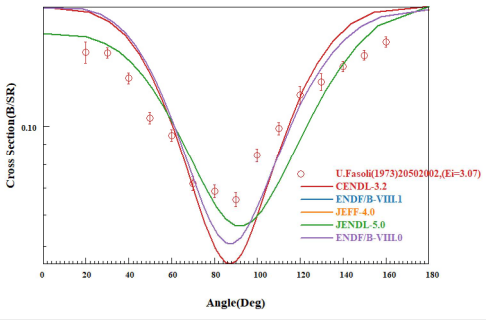

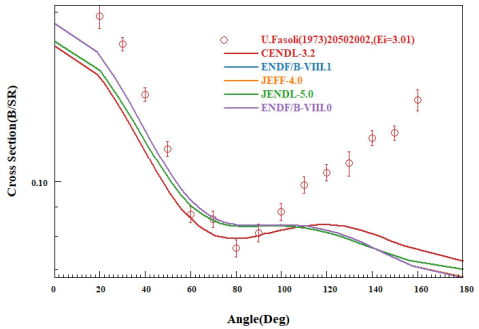

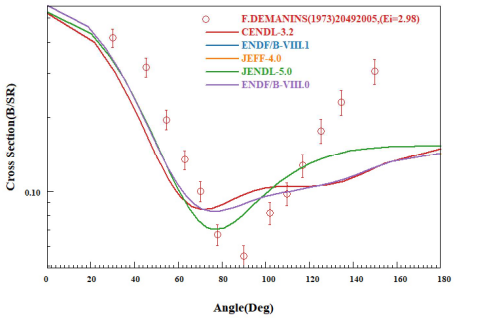

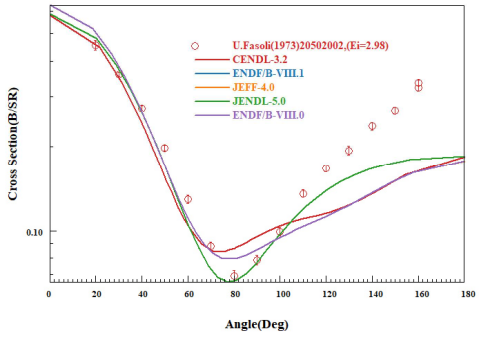

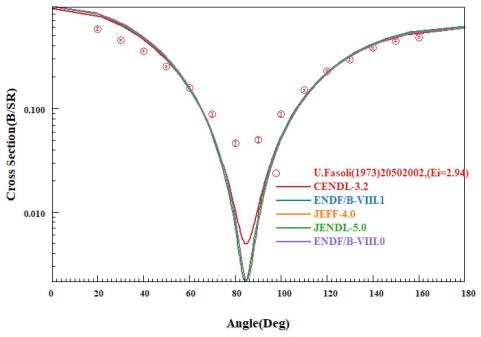

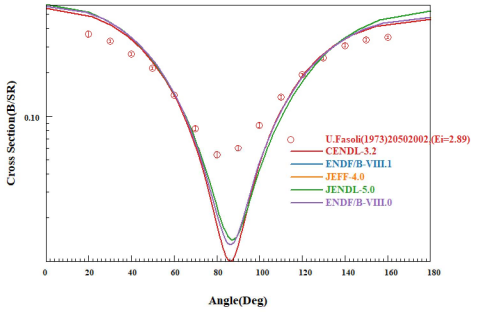

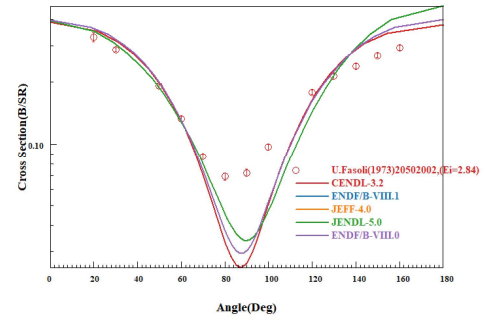

Comparison of angular distributions in the evaluation database with experimental results in the 2.84–3.71 MeV range

>20MeV

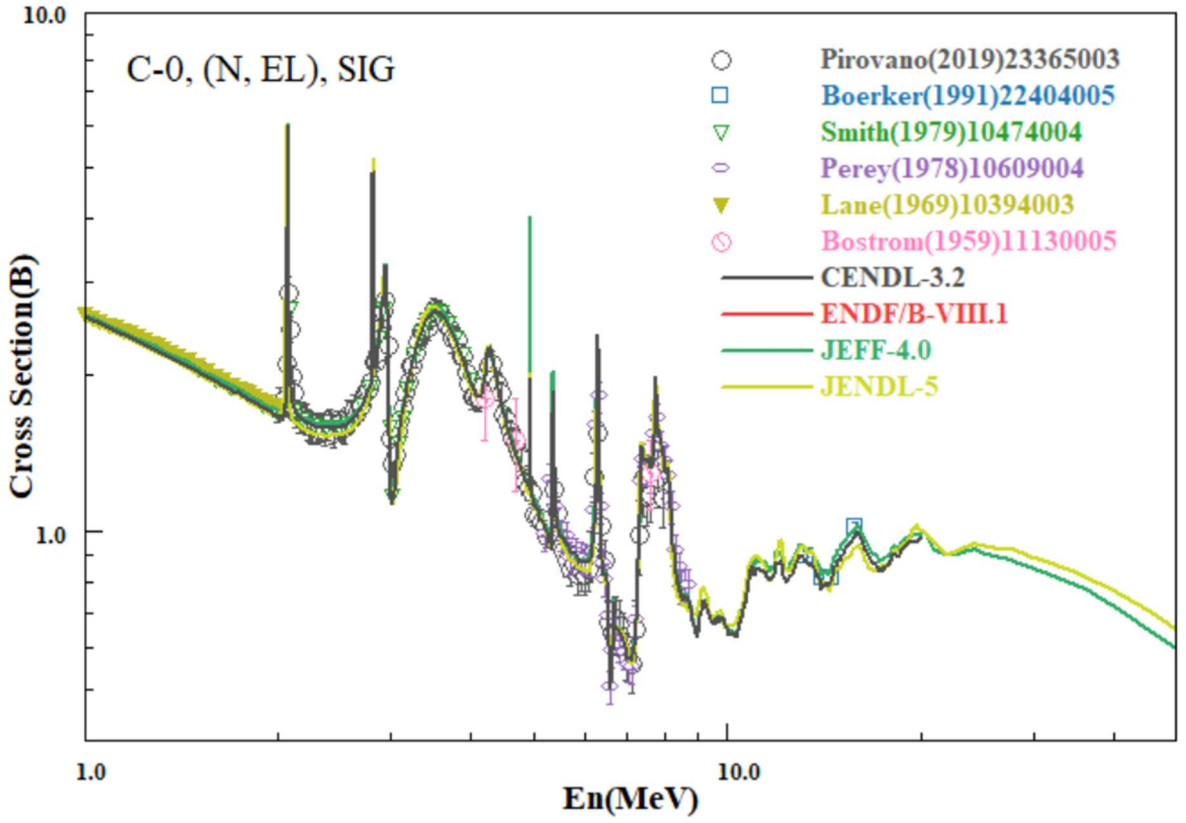

CENDL-3.2 lacks data above 20 MeV.

110 deg

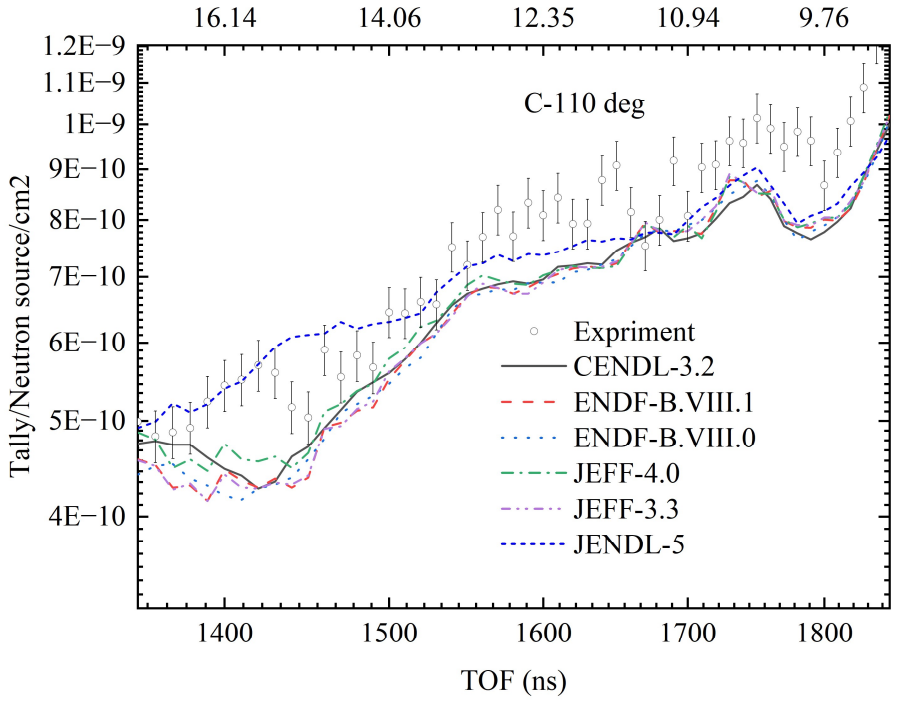

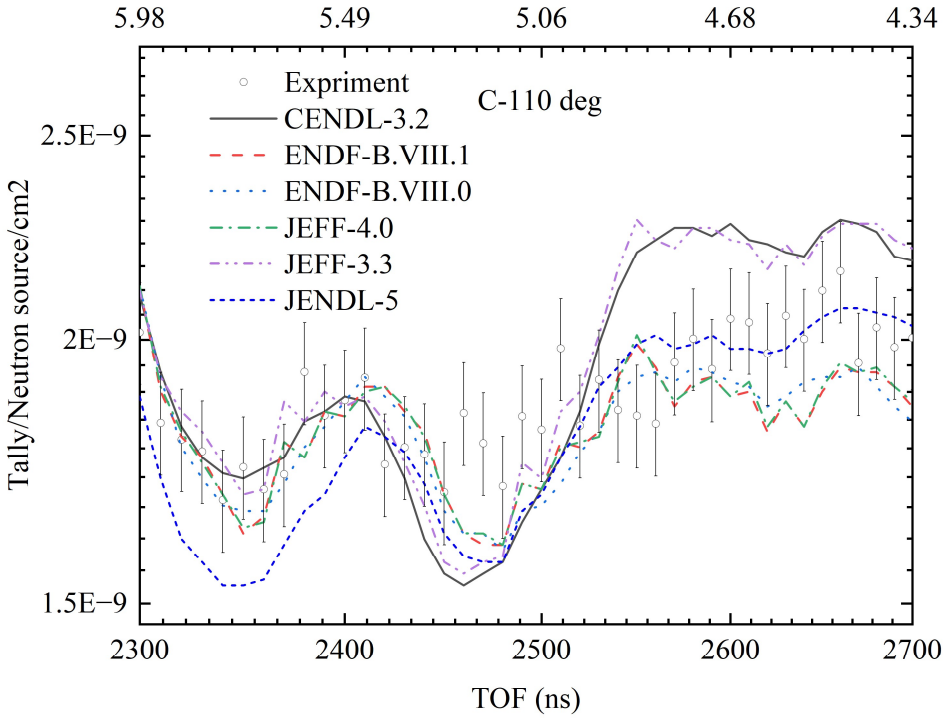

JENDL-5 provides the best C/E value within the 12–18 MeV range.

JENDL-5 exhibits the best C/E ratio within the 4.3–5 MeV range, while CENDL-3.2 performs best at 5.5–6 MeV.

JENDL-5 provides the best C/E value within the 12–18 MeV range.

15.8 MeV

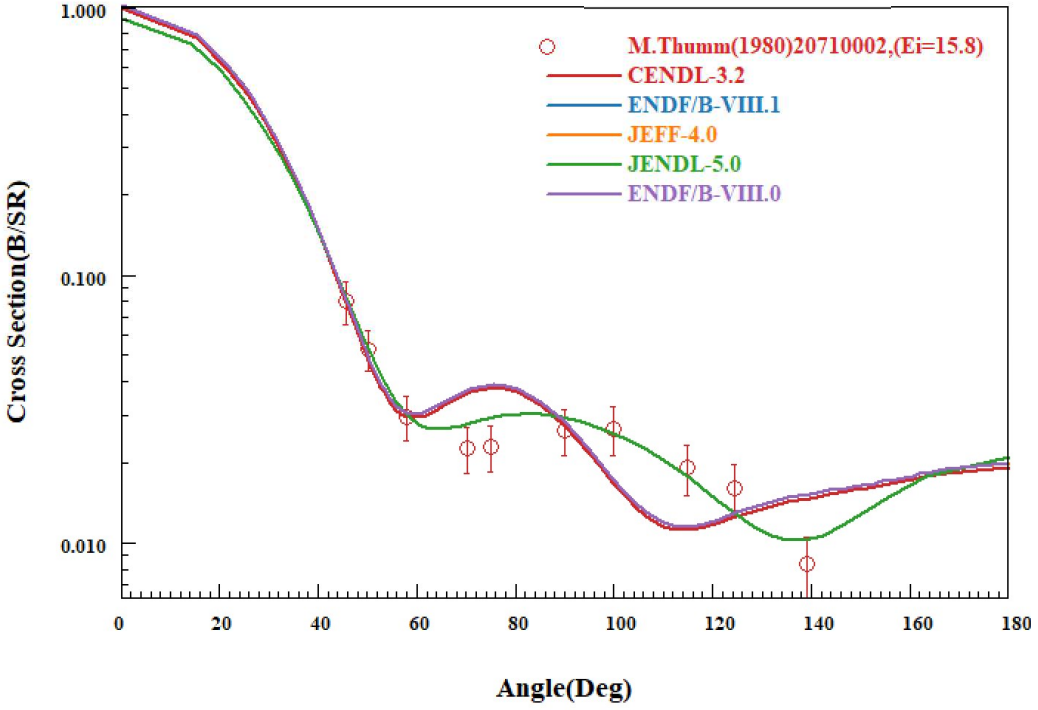

16.5 MeV

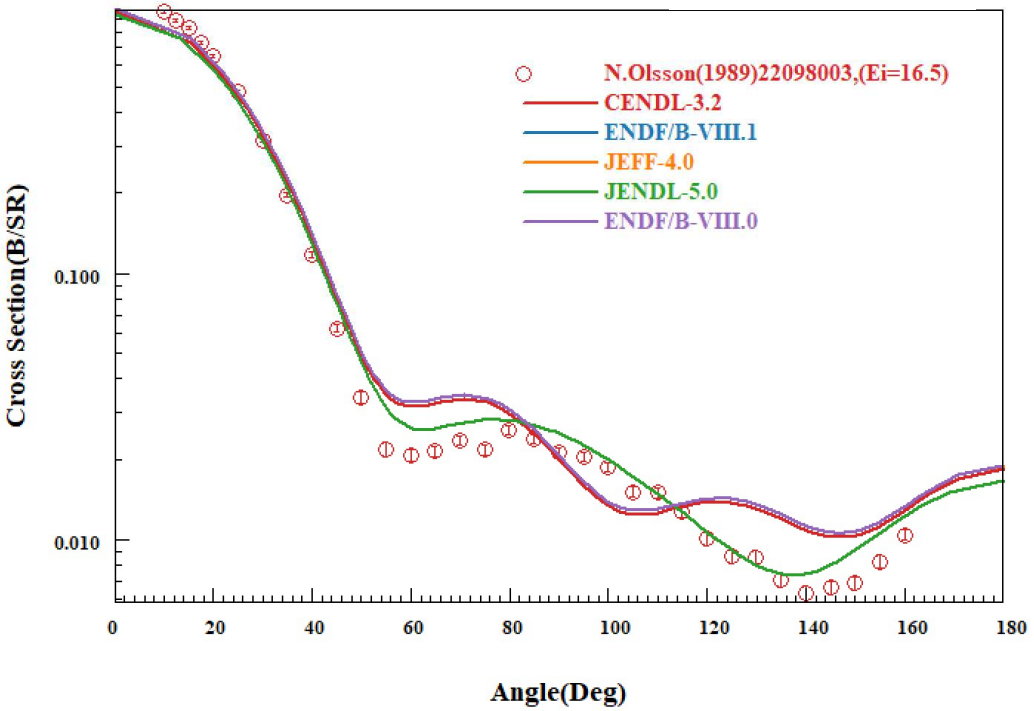

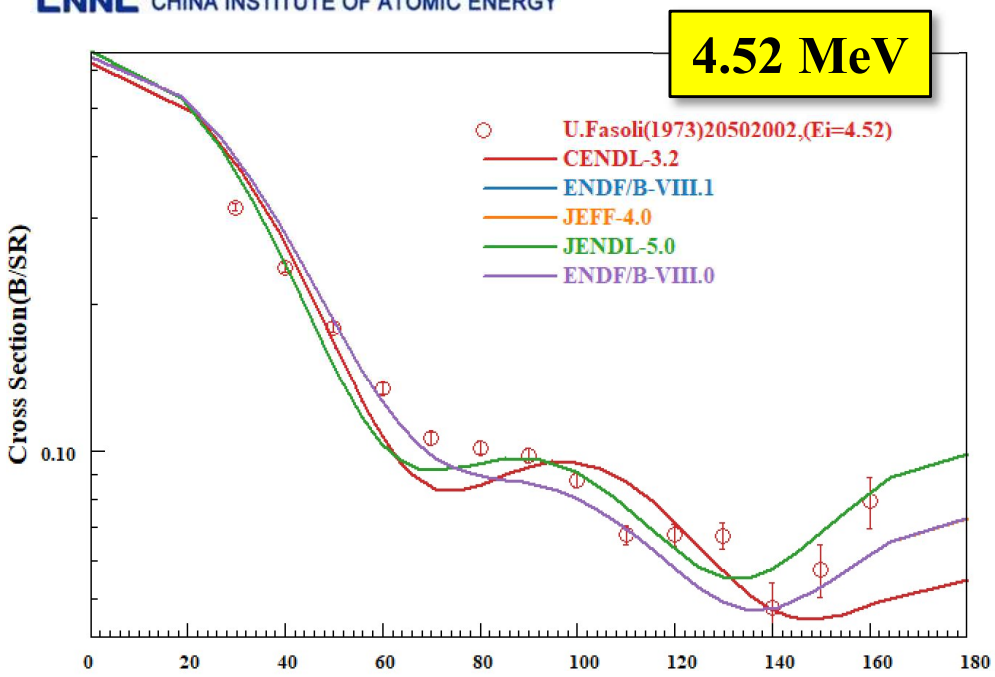

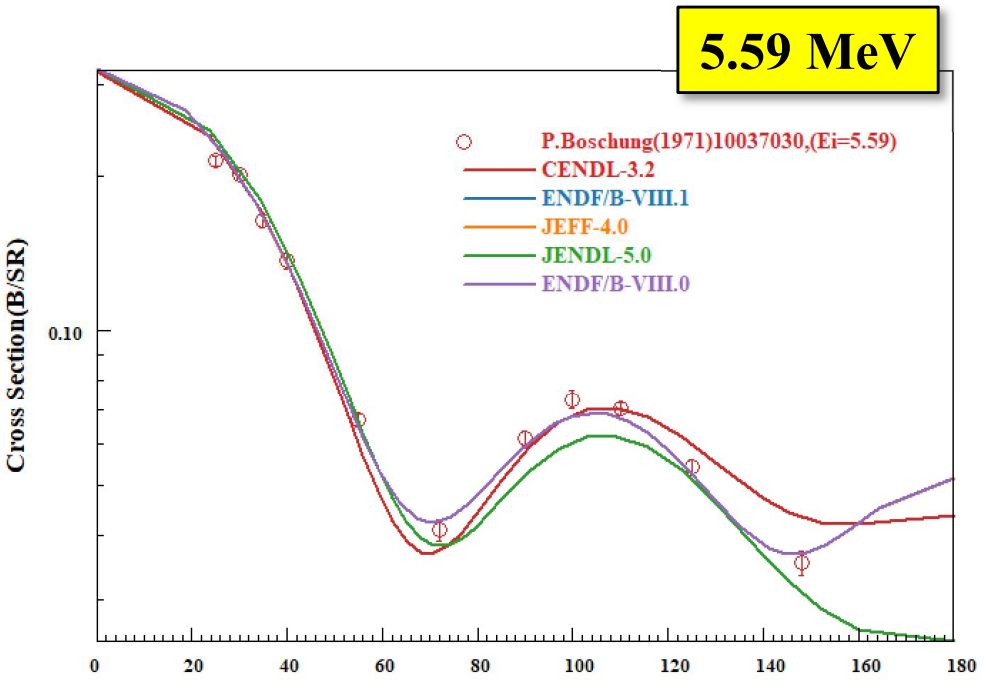

JENDL-5 exhibits the best C/E ratio within the 4.3–5 MeV range, while CENDL-3.2 performs best at 5.5–6 MeV.

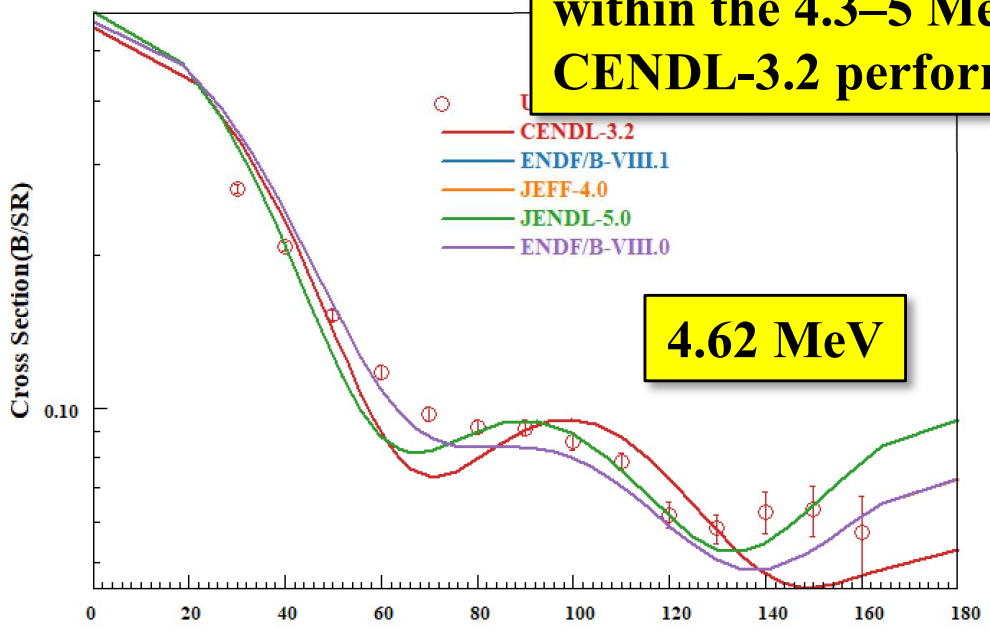

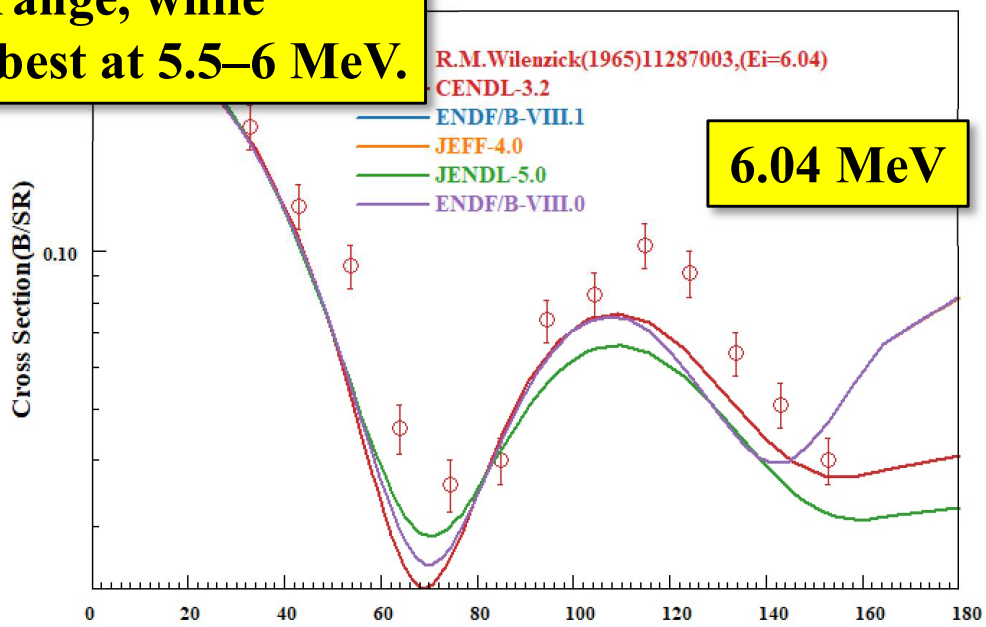

150 deg

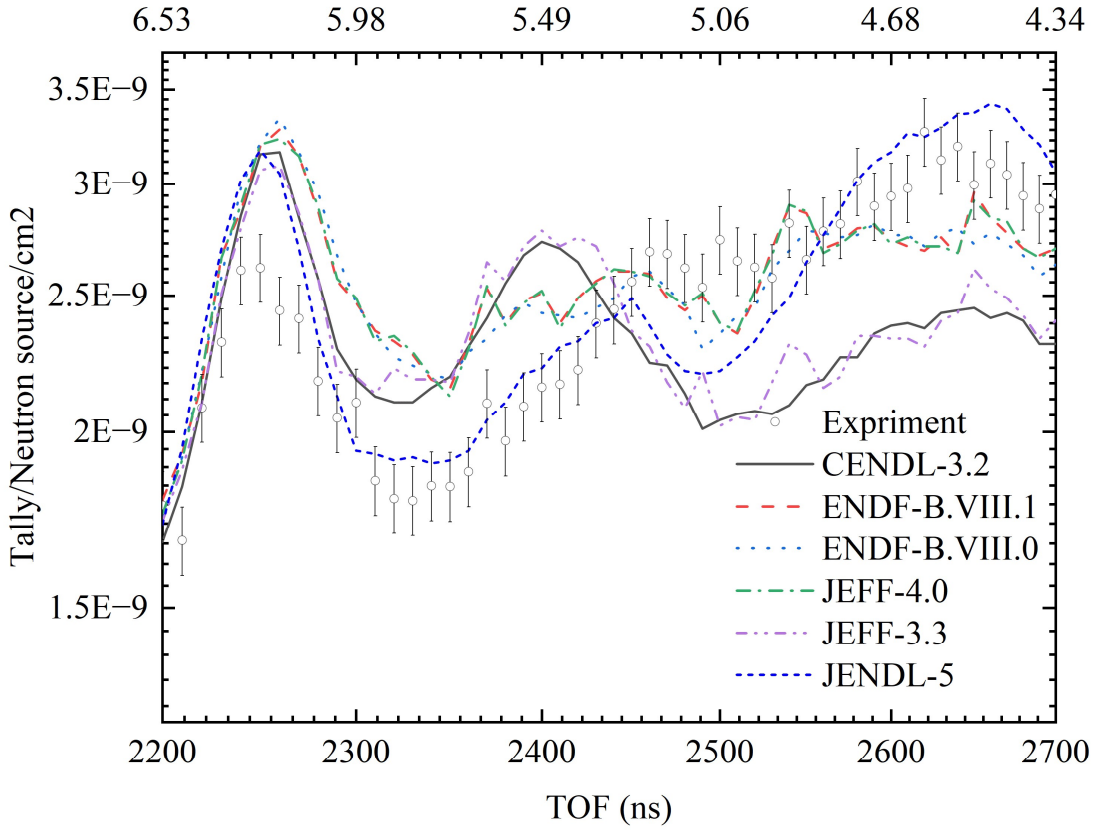

At 4.1-4.3 MeV, ENDF exhibits the optimal C/E ratio;4.3–4.8 MeV, JENDL-5 exhibits the optimal C/E ratio; at 4.8–5.2 MeV, ENDF is optimal; and at 5.2–6 MeV, JENDL-5 is optimal.

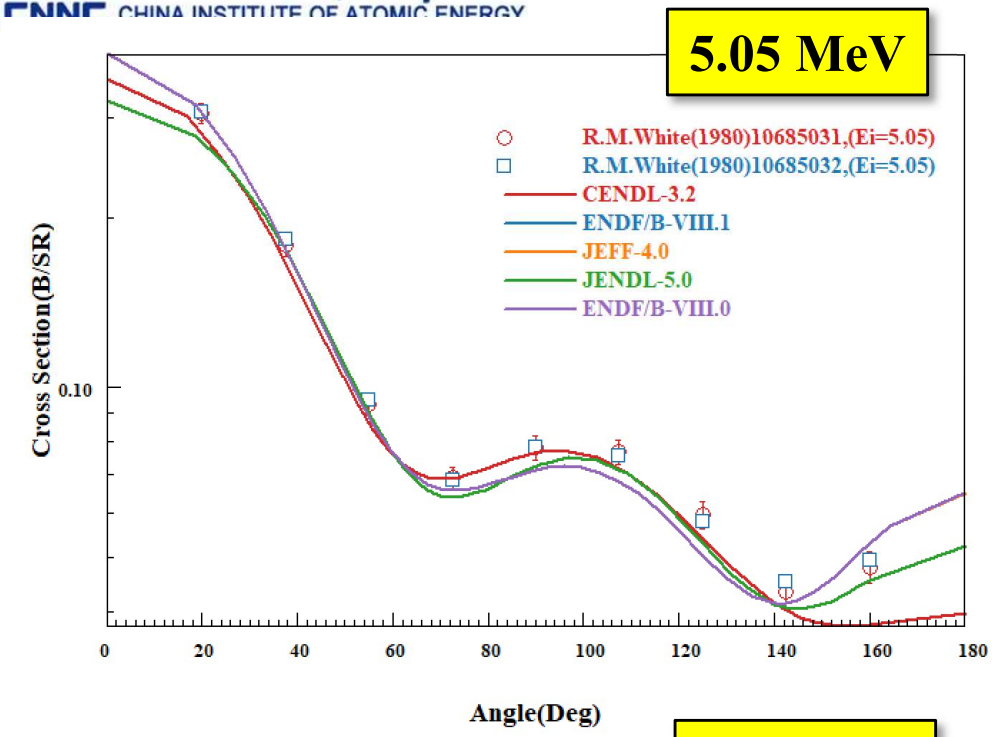
5.05 MeV
R.M.White(1980)10685031,(Ei=5.05)
R.M.White(1980)10685032,(Ei=5.05)
CENDL-3.2
ENDF/B-VIII.1
JEFF-4.0
JENDL-5.0
ENDF/B-VIII.0
Cross Section(B/SR)
0.10
0
20
40
60
80
100
120
140
160
180
Angle(Deg)

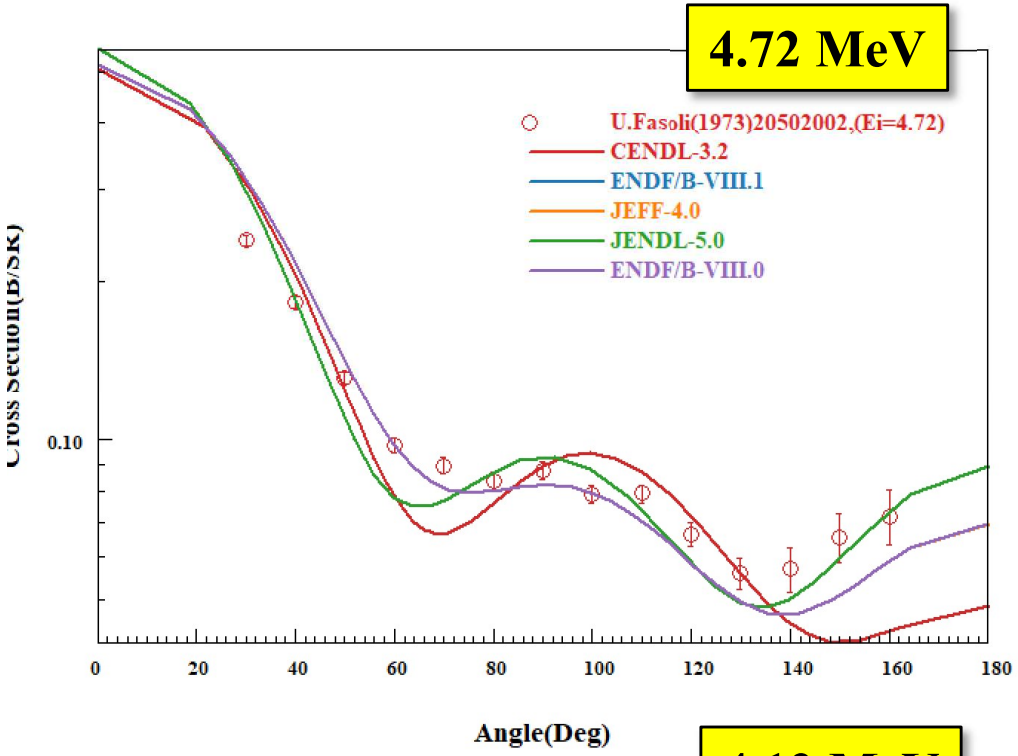
4.72 MeV
U.Fasoli(1973)20502002,(Ei=4.72)
CENDL-3.2
ENDF/B-VIII.1
JEFF-4.0
JENDL-5.0
ENDF/B-VIII.0
0.10
0
20
40
60
80
100
120
140
160
180
Angle(Deg)

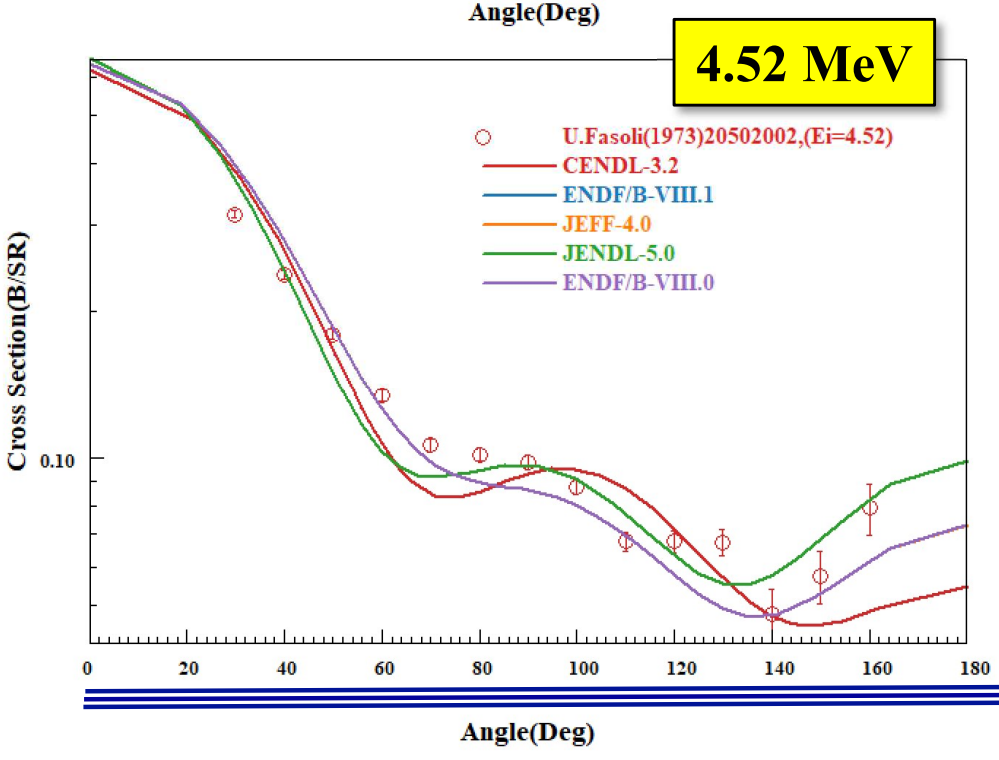
4.52 MeV
U.Fasoli(1973)20502002,(Ei=4.52)
CENDL-3.2
ENDF/B-VIII.1
JEFF-4.0
JENDL-5.0
ENDF/B-VIII.0
Cross Section(B/SR)
0.10
0
20
40
60
80
100
120
140
160
180
Angle(Deg)

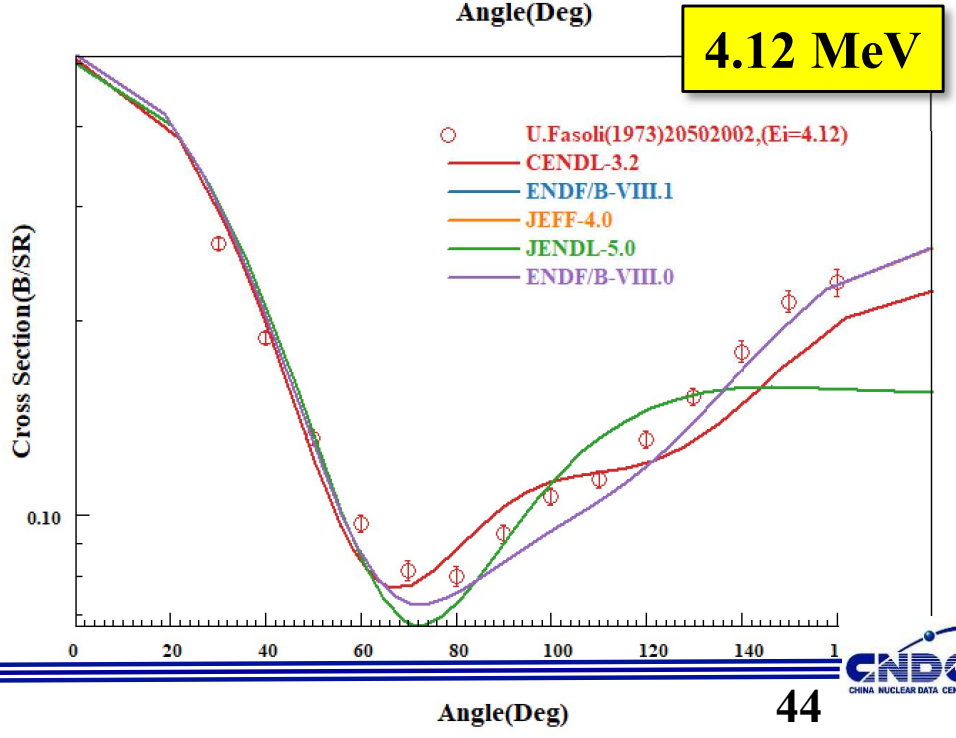
4.12 MeV
U.Fasoli(1973)20502002,(Ei=4.12)
CENDL-3.2
ENDF/B-VIII.1
JEFF-4.0
JENDL-5.0
ENDF/B-VIII.0
Cross Section(B/SR)
0.10
0
20
40
60
80
100
120
140
Angle(Deg)

n-γ discrimination with broaden the lower limit of energy threshold using BP neural network

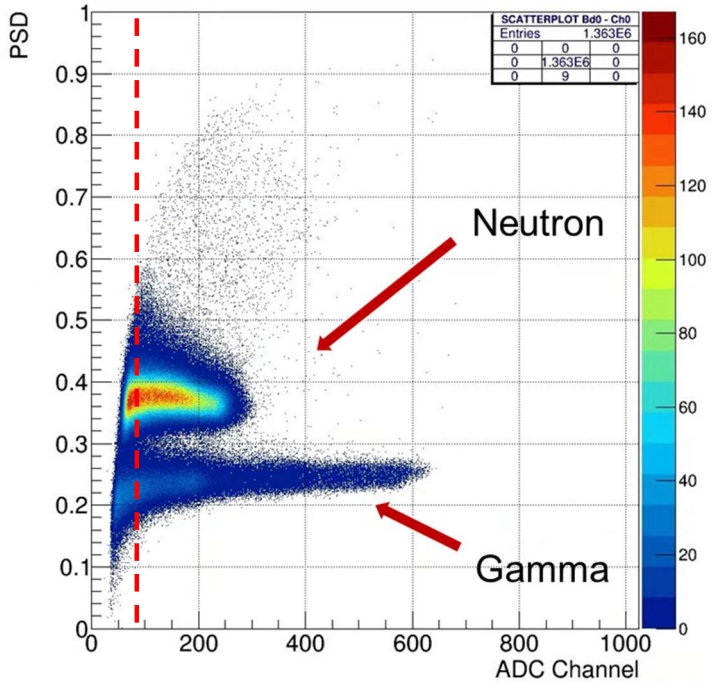

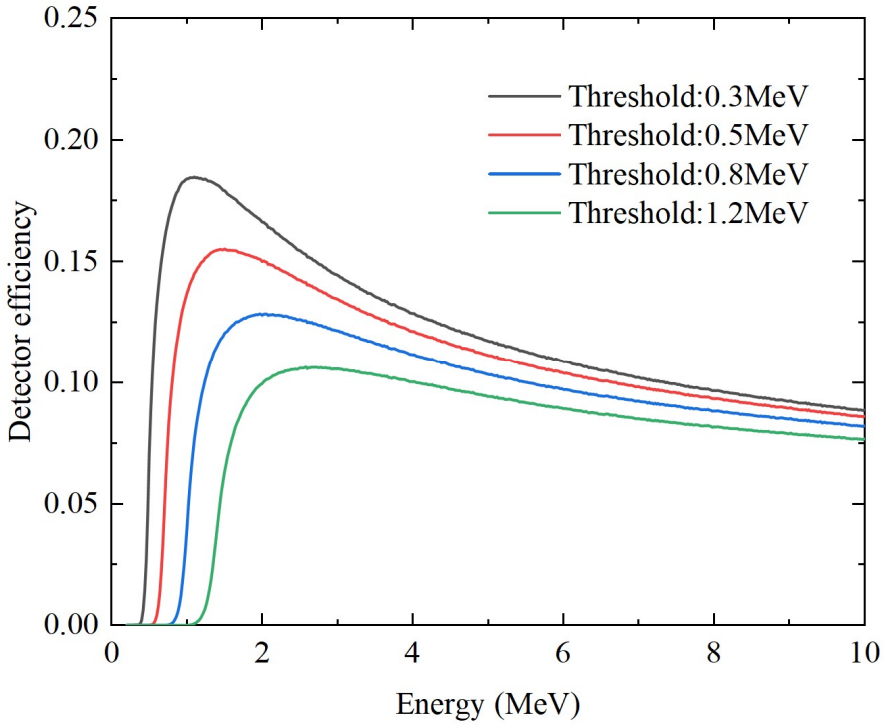

Low-energy data can enhance neutron detection efficiency.

When using the traditional PSD method, detectors have an effective detection limit.

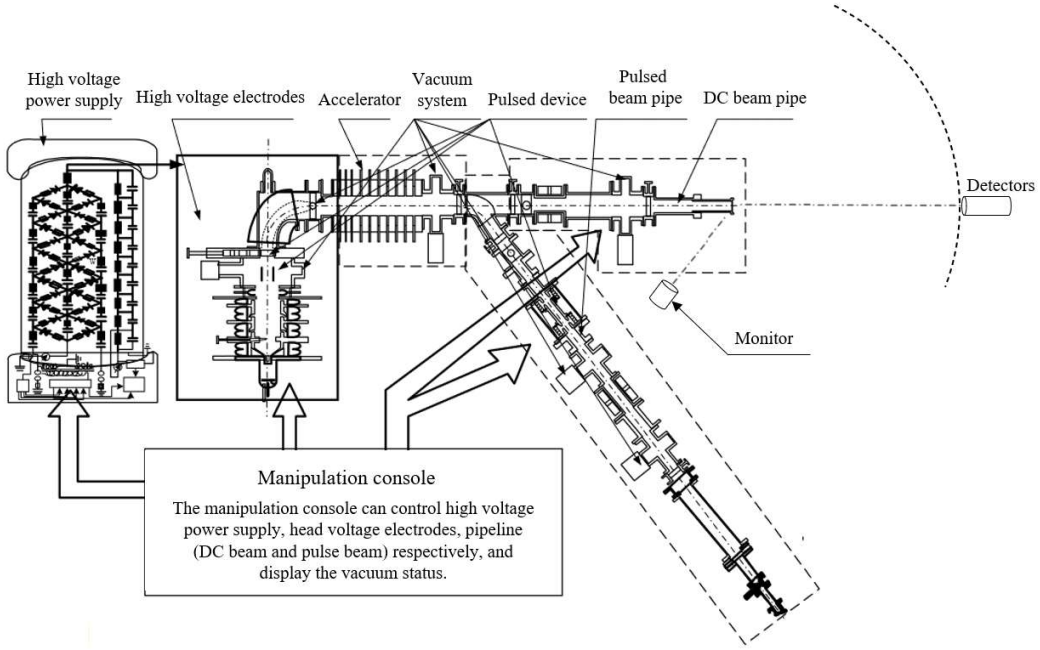

D-D Neutron Source
1m Neutron Time-of-Flight
n-γ differentiation is primarily achieved through waveform discrimination.

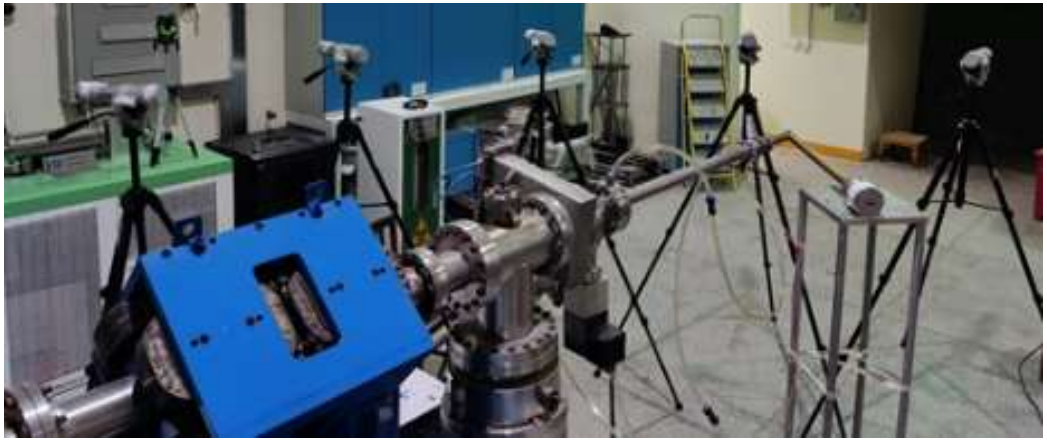

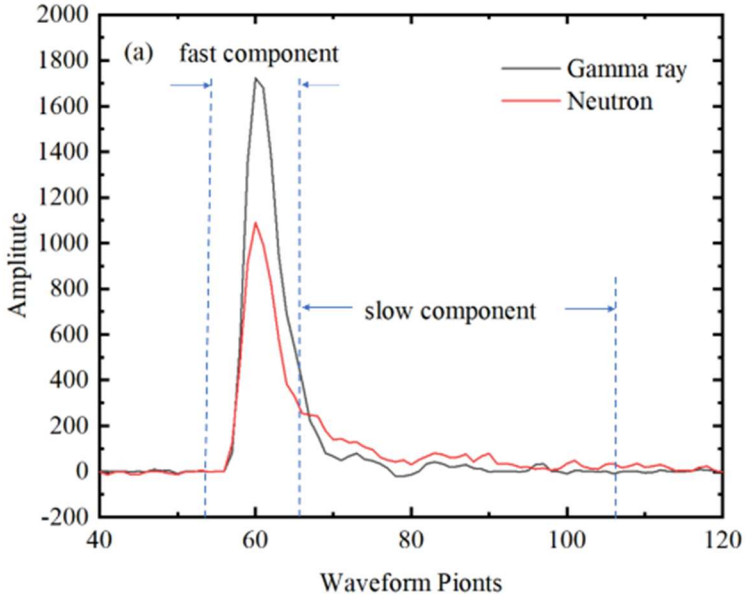

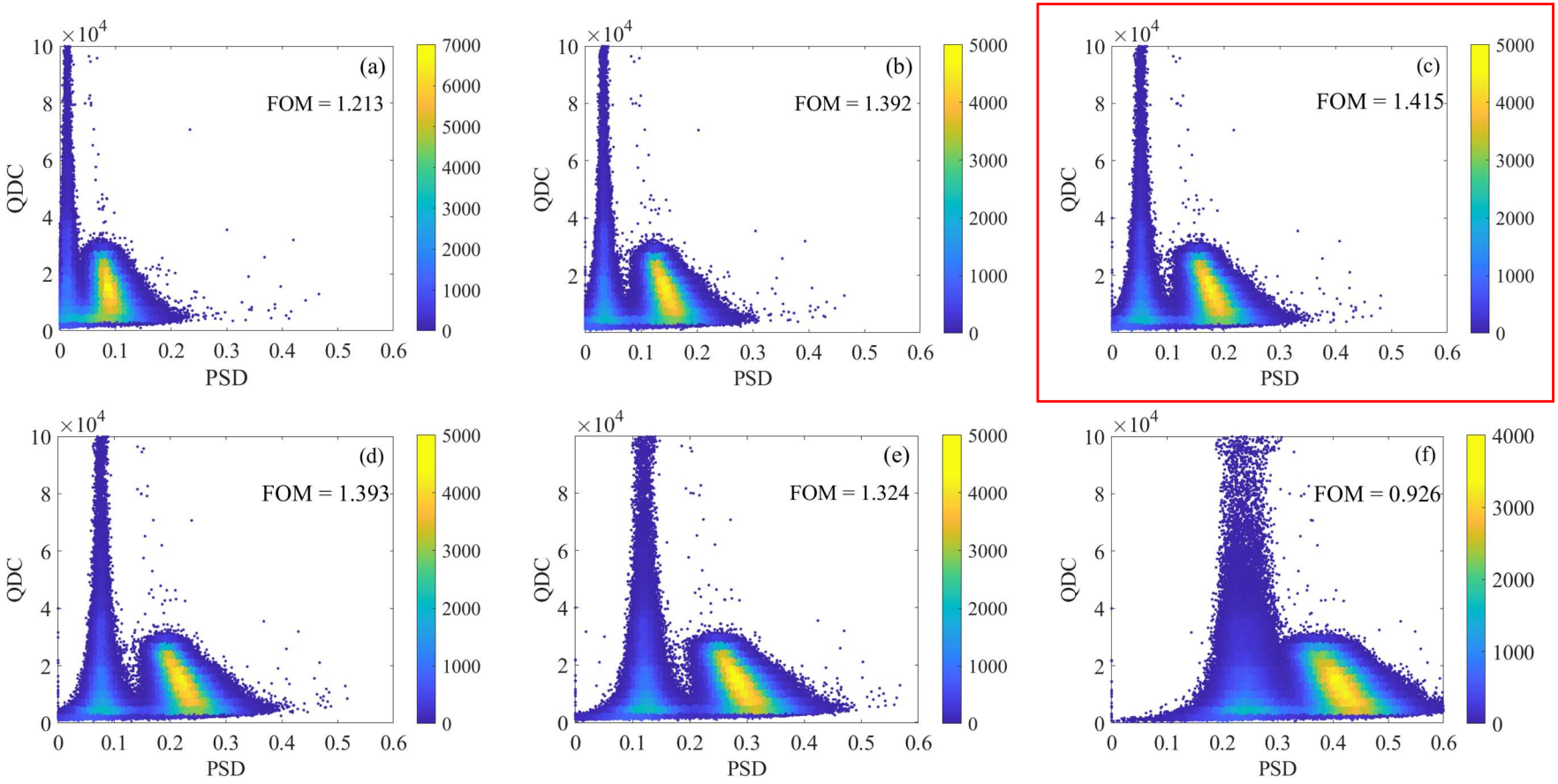

The optimal parameters of traditional PSD methods still exhibit a distinguishable lower bound.

The neural network can process all waveform information.
The outputs are neutron confidence and gamma confidence, respectively.

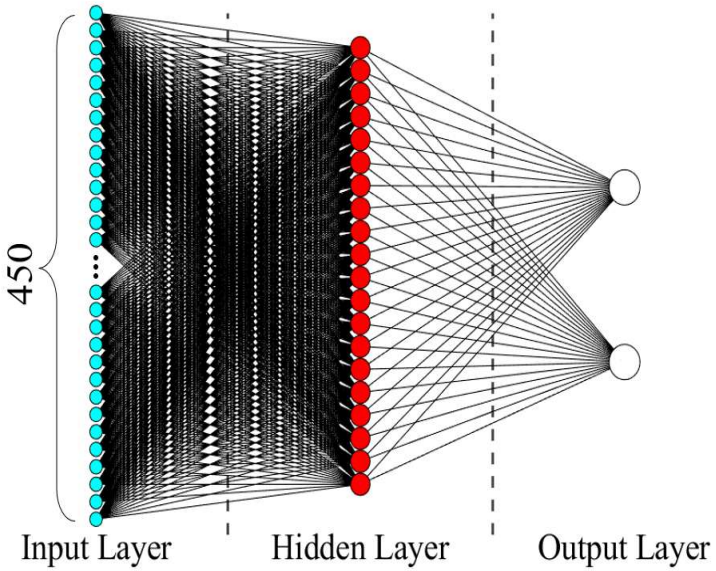

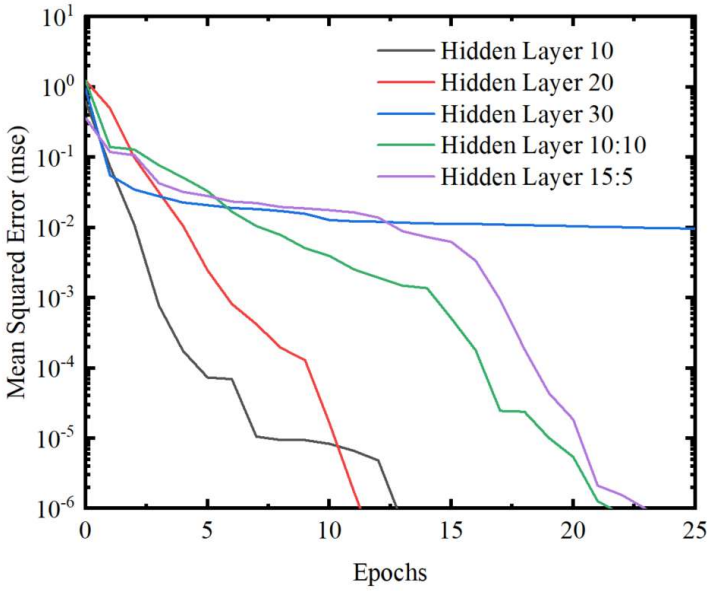

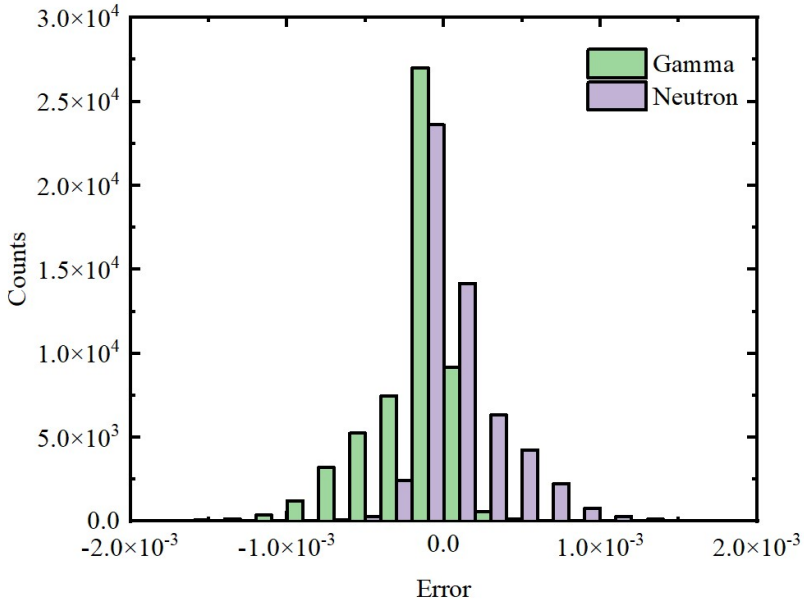

A single layer of 20 neurons yields optimal performance, with 99.9% particle confidence error below 0.02 and 100% discrimination accuracy.

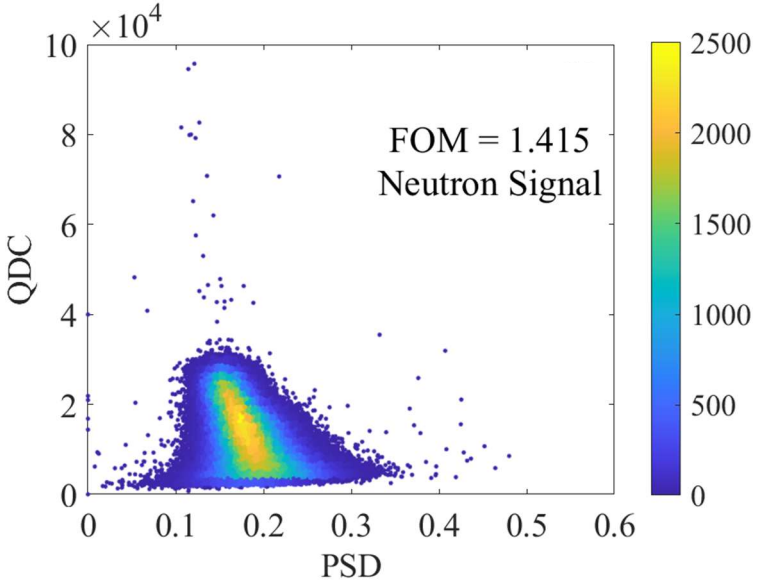

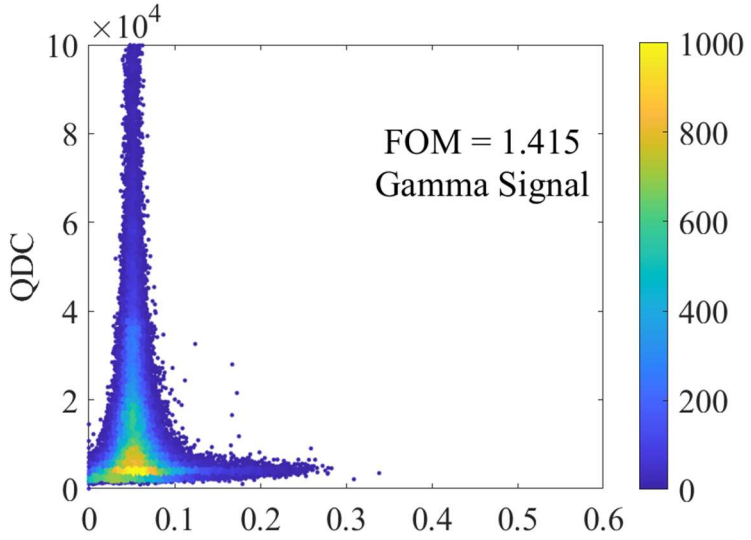

99.97% of all waveforms are distinguishable. The lower limit of distinguishable energy has been reduced from 150 keV to 70 keV. Waveform utilization rate has increased from 60% to over 99%.

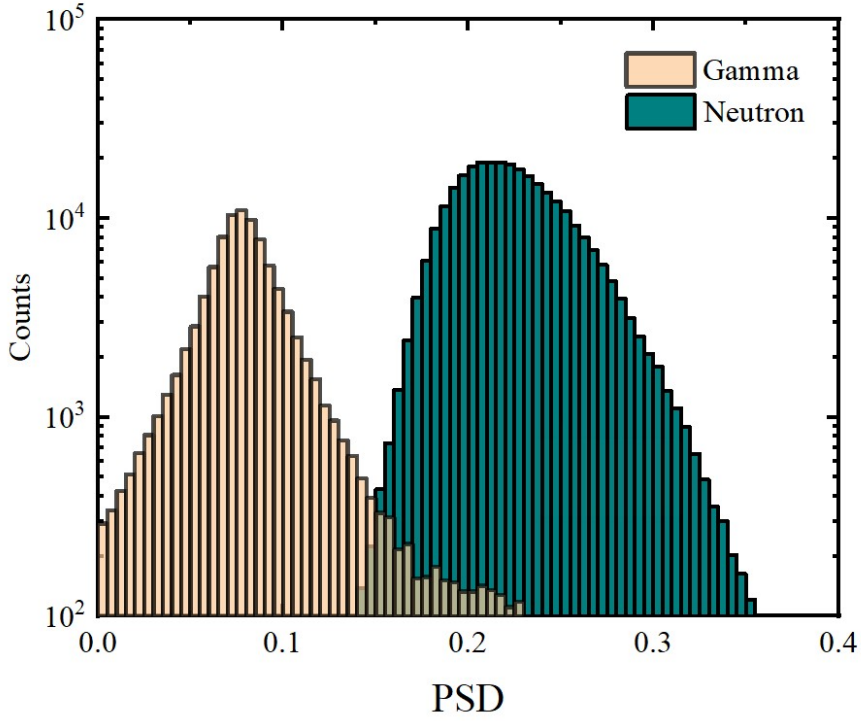

The reliability of low-energy resolution differentiation based on TOF spectrum identification.

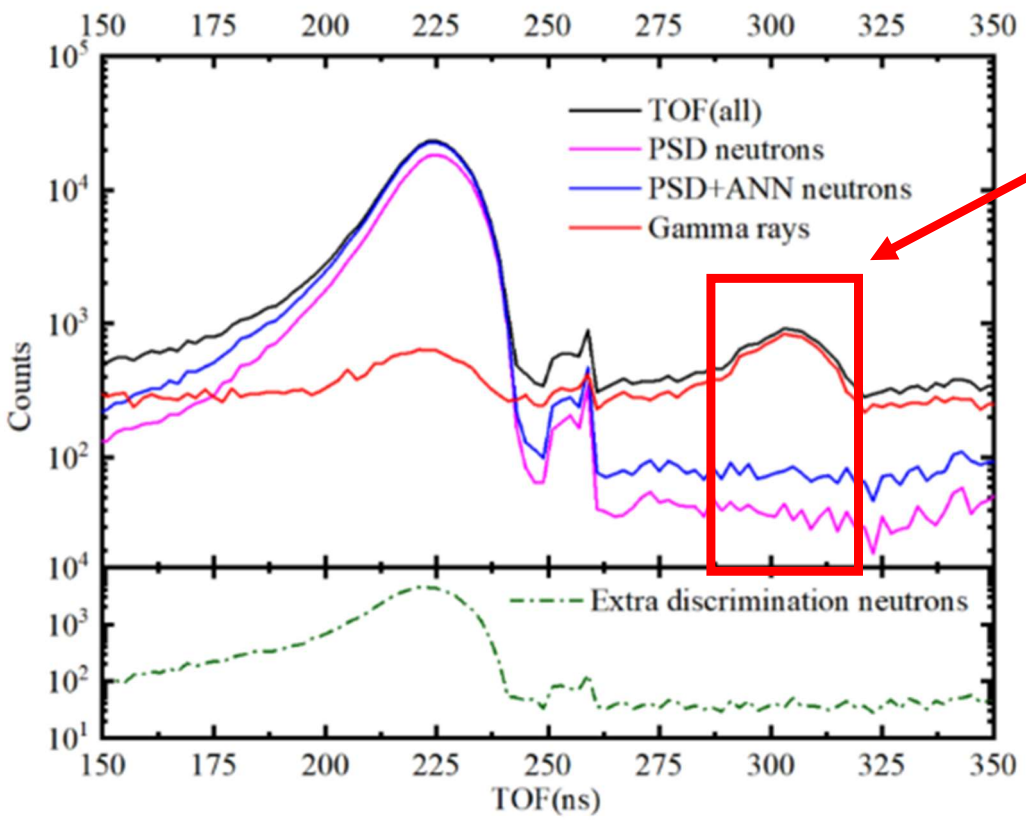

γ-flash

No neutrons are present at the γ-flash peak.
A γ peak exists at the neutron peak.
The TOF spectrum shapes for low-energy neutrons are consistent.

TOF in Reverse

Verification of the PSD-ANN Method's Universality.

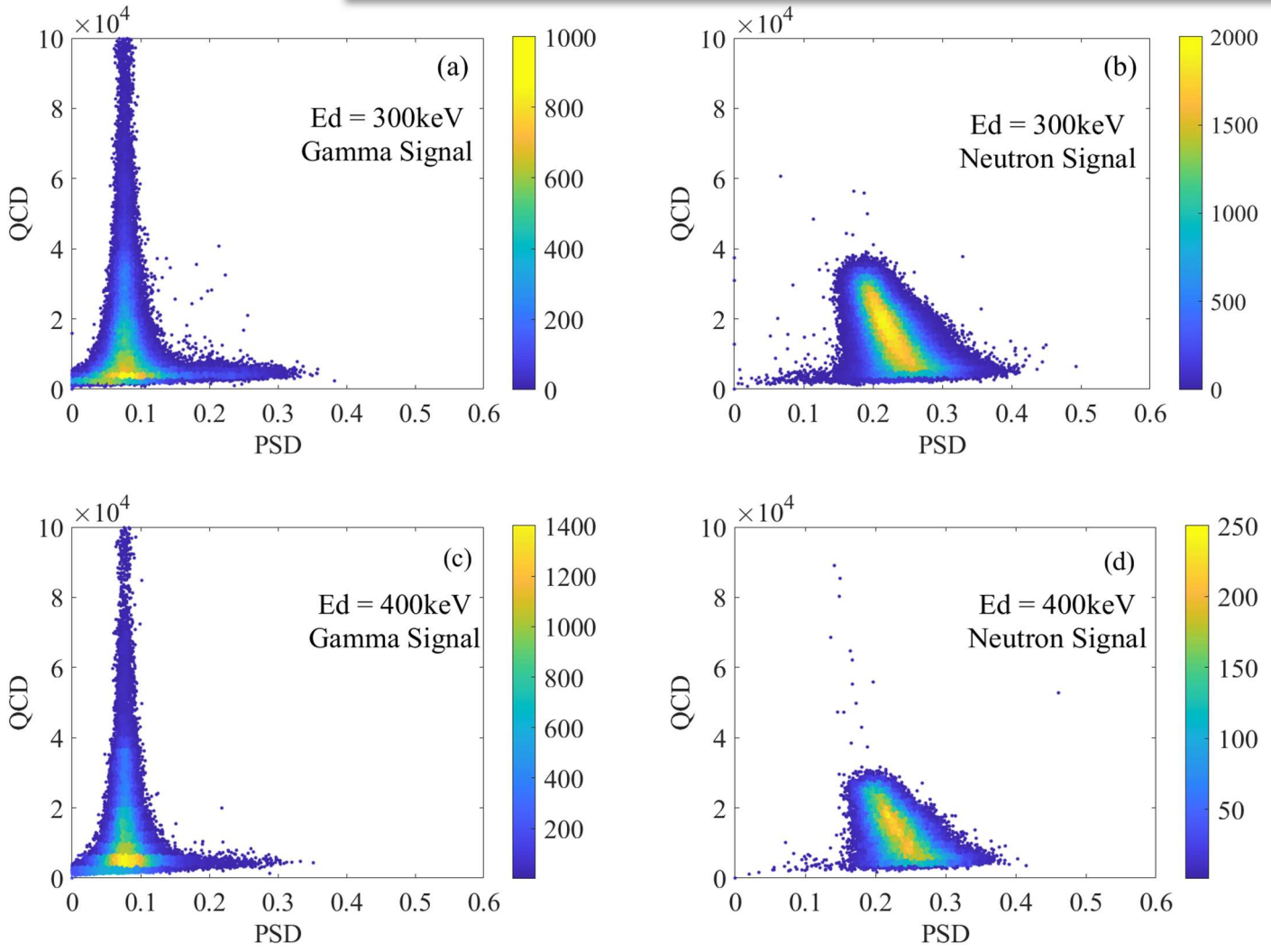

After fixing the detector and acquisition system.

For a pre-trained neural network, Real-time discrimination can be achieved in experiments.

Summary

1. The CIAE's integral experimental platform is now capable of precisely measuring the neutron leakage spectrum from plate-shaped/spherical experimental samples under D-T/D-D neutron source conditions.
2. Experimental data for Bi still requires further refinement: **under D-T neutron sources**, elastic scattering data aligns best with CENDL-3.2, while (n, 2n) reactions perform optimally with JENDL-5. Notably, after updating to JEFF-4, the JEFF library shows consistency with JENDL-5 data, though JEFF-3.3 demonstrated superior performance among the six databases for continuous-energy inelastic scattering. **For D-D neutron sources,** the elastic scattering ENDF library performed best. The discrete-level inelastic high-energy region was underestimated by CENDL-3.2, but it performed best in the low-energy region.

Summary

3. Standard sample verification work has been completed using both **the CF-252 shielding experimental** platform and the **Quasi-Differential experimental** platform based on CSNS back-n, establishing the experimental conditions for sample verification.
4. The standard cross sections and angular distributions for elastic scattering of C show good performance within the range recommended by the IAEA, but significant discrepancies remain in the angular distribution above 1.6 MeV.
5. A method for distinguishing n-γ in the low-energy region of liquid scintillation detectors has been developed. The lower limit of distinguishable energy has been extended using neural networks, and reliability has been verified using time-of-flight measurements.

Thank you for your attention !